Spring 1-1-2010

Tertiary cooling history of the Gore Range: a northern Rio Grande Rift flank uplift, central Colorado

Rachel Landman
University of Colorado at Boulder, rachel.landman@gmail.com

Tertiary cooling history of the Gore Range: a northern Rio Grande Rift flank uplift, central Colorado

By

Rachel Landman

B.A., Amherst College, 2007

A thesis submitted to the

Faculty of the Graduate School of the

University of Colorado in partial fulfillment

of the requirement for the degree of

Master of Science

Department of Geological Sciences

2010

Signature Page

This thesis entitled:
Tertiary cooling and unroofing of the Gore Range: a northern Rio Grande Rift flank uplift, central Colorado
written by Rachel Landman
has been approved for the Department of Geological Sciences

____
Dr. Rebecca Flowers

____
Dr. Craig Jones

____
Dr. Karl Kellogg

Date_______________

The final copy of this thesis has been examined by the signatories, and we Find that both the content and the form meet acceptable presentation standards Of scholarly work in the above mentioned discipline.

Landman, Rachel (M.S., Department of Geological Sciences)
Tertiary cooling history of the Gore Range: a northern Rio Grande Rift flank uplift, central Colorado

Thesis directed by Assistant Professor Rebecca M. Flowers

ABSTRACT

Despite extensive study, there is no consensus on why or when the Rocky Mountains experienced the uplift that created the region’s dramatic topography. Some infer that the region experienced regional uplift as recently as the last few million years, possibly attributable to mantle upwelling associated with the Rio Grande Rift. Whether the Rift propagated northward in Tertiary time as implied by its tapering northward character or experienced a similar history along most of its length bears on the role of the Rift in the evolution of the Rockies. The Gore Range and adjacent Blue River Valley of central Colorado represent the northernmost significant fault-related manifestation of the Rift in the heart of the Rockies. The Blue River normal fault separates the basin from the range and accommodates a minimum vertical displacement of 1.2 km, creating 1.4 km relief in the entirely crystalline southern half of the range. A cross fault separates the southern from the northern Gores. The rolling hills north of the cross fault have a maximum relief of 700 m, vertical displacement on the Blue River fault of up to 800 m, and retain a partial cover of Mesozoic sedimentary and mid-Tertiary volcanic rocks.

Apatite (U-Th)/He dates for 15 samples in the southern Gore Range are younger eastward toward the Blue River fault. In the western Gore Range, Eocene dates are preserved at elevations >3600 m while Oligocene dates occur at lower elevations. Eastern Gore samples from an elevation range of 4000-3000 m yield Miocene dates. The youngest date of 6.9 Ma occurs at an elevation of 2790 m at the eastern edge of the range. These results suggest two separate cooling and unroofing episodes in Oligocene and Miocene time. The youngest date implies ~2 km of unroofing in the easternmost Gore Range since the late Miocene. It is inferred that the entire range underwent late Oligocene unroofing. The geomorphic contrast between the northern and southern Gores is likely due to the restriction of significant displacement along the Blue River fault to the southern Gores, inducing Miocene unroofing, creating significant relief, and stripping any remaining sedimentary cover from this area. This two-phase unroofing history is similar to that inferred for other rift basins to the south, implying the broadly synchronous onset and evolution of a >700 km segment of the Rio Grande Rift.

Acknowledgements

First of all, I have to thank Becky Flowers. Thanks for giving me a fascinating project in a gorgeous part of the world, and for your enthusiasm and encouragement as I worked through the research process and tried to understand what it all meant. I've been lucky to get to observe both your dedication and your work ethic – you are a role model. Thanks also to Charles Naeser for so generously sharing all of his mineral separates from the Gore Range. And to Karl Kellogg for kindly sharing his unpublished Gore Range map, making my fieldwork so much more effective, and to Craig Jones for serving on my committee and bringing a different perspective to the project.

Funding for this work was provided by grant #47476 to Rebecca Flowers from the American Chemical Society Petroleum Research Fund. Additional support came from graduate student research grants from Amherst College, ExxonMobil, and the Geological Society of America. Thanks also go to Alexis Ault for all the discussions in the lab, and to Ryan Nell, Nathan Rogers, and Andy Wickert for all the help in the field. And an extra thanks to Nate – for your unwavering support.

Table of Contents

List of Tables

List of Figures

1. Introduction

Geologists have studied the Colorado Rockies for well over a century. Yet there is still no clear understanding as to why the region was uplifted, when this happened, or of the tectonic and geomorphic processes that formed both the high elevation and high relief in the region. Some studies present paleobotanical evidence to suggest that the Rockies reached their current elevations during Early Tertiary contraction with subsequent exhumation the product of climate change (e.g., Gregory and Chase, 1992). Others have used the tilt of reconstructed basin fill surfaces to infer that the Rocky Mountain region underwent epeirogenic elevation gain as recently as 8-5 Ma, possibly caused by a mantle anomaly that manifests at the surface as the Rio Grande Rift system (McMillan et al., 2002, 2006; Leonard, 2002).

The Rio Grande Rift extends over 1,000 km from Mexico into central Colorado and the heart of the southern Rocky Mountains (Figure 1). A clear understanding of the spatial and temporal evolution of the rift is necessary to evaluate hypotheses that link the evolution of the rift with Late Tertiary uplift of the Rockies. The rift's tapering northward character has led to a widespread assumption that rifting initiated in the south and then propagated north into Colorado over time. However, studies of rift basins from central New Mexico and southern Colorado suggest that onset of rifting was broadly coeval at ~29-26 Ma from at least the Socorro Basin northward through the San Luis Basin, and probably into the Upper Arkansas Basin as well (e.g., Chapin and Cather, 1994). The Upper Arkansas Basin is the northernmost of the major rift basins containing deep Tertiary fill (Figure 2; Tweto, 1979). Basins lacking that fill but sharing other structural similarities with the rift basins extend north to the Wyoming border (Kellogg, 1999). We refer to these northern basins as the "northern Rio Grande Rift." It remains an open question whether the northern basins developed as the Rift propagated northward into southern Colorado, or if they evolved over a similar time frame as the more significant basins to the south.

The Gore Range in central Colorado bounds one of the northernmost grabens of the Rio Grande Rift. The Blue River normal fault separates the Blue River Valley from the range and accommodates a minimum vertical displacement of 1.4 km, creating 1.4 km of relief in the southern half of the range. The dramatically carved Gore Range stands out from the neighboring and lower relief western Front Range and Park Range. The Gore Range proves similarly distinctive when evaluating patterns of apatite fission-track (AFT) dates in the southern Rockies (Figure 2). Mid- to Late Tertiary AFT dates for the Gore Range (Naeser et al., 2002) contrast with Late Cretaceous and Early Tertiary results from adjacent areas. Apatite (U-Th)/He thermochronometry is sensitive to lower temperatures (~70-30 °C) than the AFT technique, making it potentially an ideal tool to better constrain the Mid- and Late Cenozoic cooling history of the southern Rocky Mountains, yet no apatite (U-Th)/He data has been published from this region. This study presents apatite (U-Th)/He data for fifteen samples from the southern Gore Range. The results are used to decipher the Mid- and Late Tertiary cooling and unroofing history of this northern segment of the Rio Grande Rift. This history is then compared with the evolution of better-studied basins to the south, and the first-order implications for the overall development of the Rio Grande Rift system are considered.

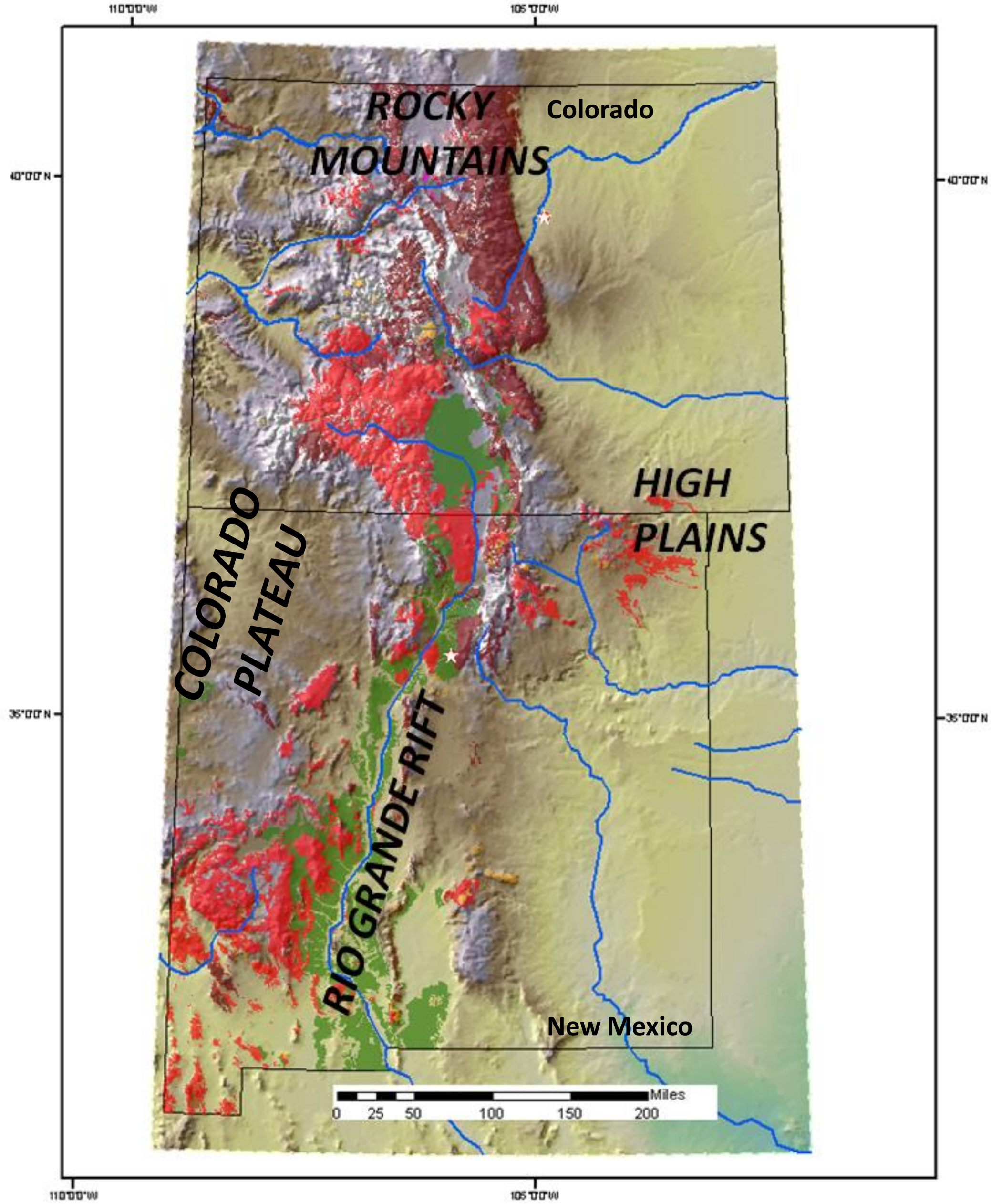

Figure 1: Topography of the Rio Grande Rift and southern Rocky Mountain region depicting the distribution of Proterozoic basement, Tertiary intrusive and volcanic rocks, and Oligocene-Pliocene synrift deposits.
Geologic maps from Green, 1992; Green and Jones, 1997.

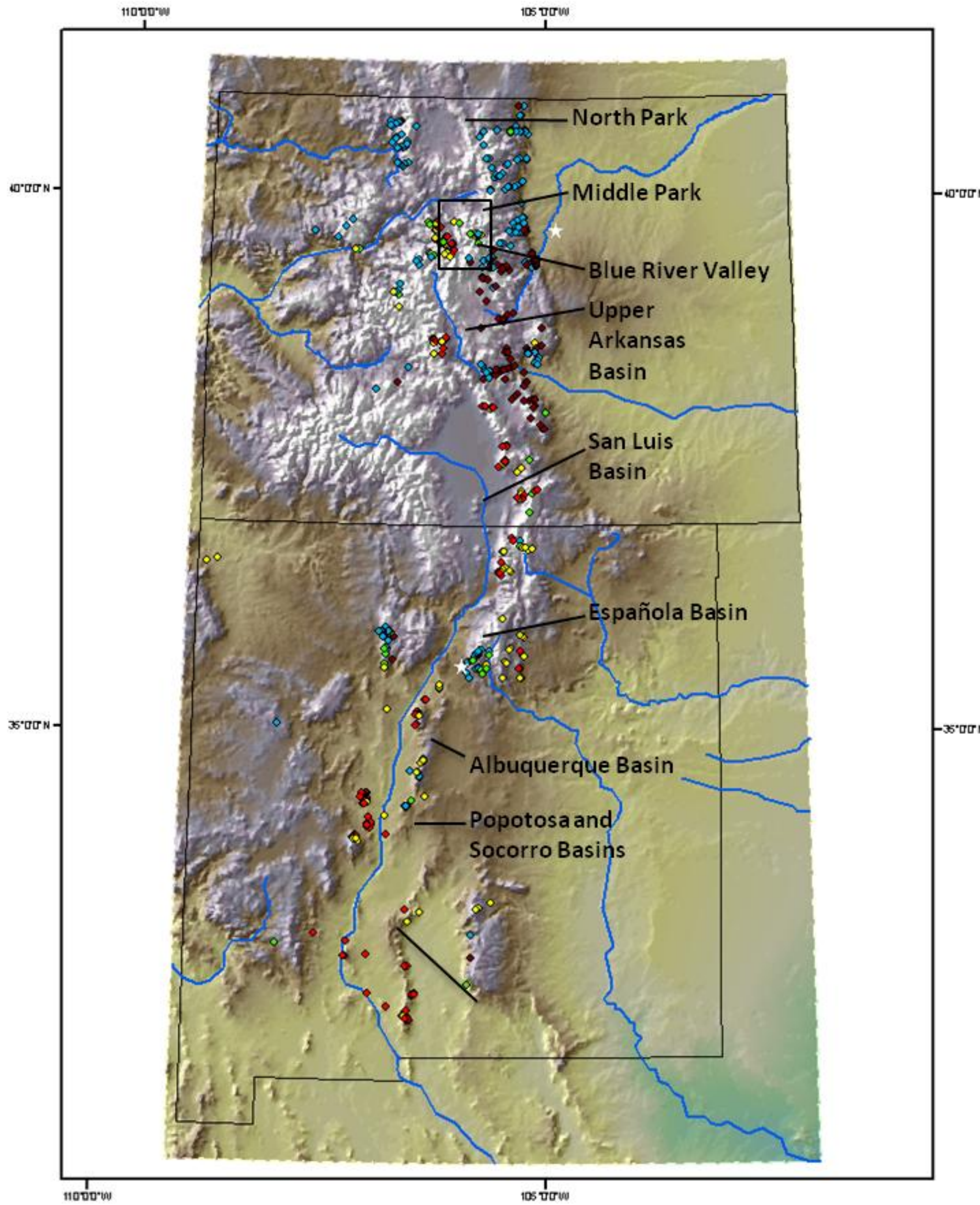

Figure 2: Apatite fission-track dates for the Rio Grande Rift and southern Rocky Mountain region. Black box is the boundary of Figure 3. Dates from Bryant and Naeser, 1980; Bryant et al, 1990; Church and Bickford, 1971; House et al, 2003; Kelley and Duncan, 1986; Kelley et al, 1992; Kelley and Chapin, 1995; Kelley and Chapin, 1997; Kelley and Chapin, 2004; Kelley, 2005; Lindsey et al, 1986; Lipman et al, 1986; Marvin and Dobson, 1979; Naeser, 1971; Naeser et al, 1990; Naeser et al, 2002; Olson et al, 1977; Shannon, 1988; Wilks and Chapin, 1997.

Apatite fission-track date:
- Younger than 20 Ma
- 30 – 20 Ma
- 45 – 30 Ma
- 75 – 45 Ma
- Older than 75 Ma

2. Geologic Setting

The southern Rocky Mountains are a north-northwest trending set of ranges that extend from New Mexico through Colorado and into southern Wyoming. Highest elevations are in central Colorado. The mountains sit between two geologic provinces that have been more stable throughout the Phanerozoic – the Colorado Plateau to the west and the Great Plains to the east. The Rio Grande Rift bisects the southern Rockies and is a product of the change from the contractional environment of the Laramide orogeny to an extensional regime that has dominated the region during the Late Cenozoic.

The Rio Grande Rift system is an intracontinental extensional zone that stretches from Chihuahua, Mexico, north through Texas and New Mexico and then into central Colorado (Chapin and Cather, 1994; Keller and Baldridge, 1999). Extensional basins containing deep Tertiary fill occur as far north as the Upper Arkansas Basin and valleys lacking that fill extend north into Wyoming (Tweto, 1979; Kellogg, 1999), where the Cheyenne Belt divides the Paleoproterozoic basement of Colorado from the Archean Wyoming craton. Volcanics as young as 8 Ma occur in the Elkhead Mountains near the Wyoming border (Tweto, 1979). The 2004 LA RISTRA seismic imaging study (West et al., 2004; Wilson et al., 2005) mapped crust and mantle characteristics along a transect in central New Mexico that included the rift and the adjacent Great Plains and Colorado Plateau. Results indicated that the rift is characterized by a high heat flow of 90 mW/m^2 and crust that is 10-15 km thinner than adjacent regions. Lithospheric thickness is ~50 km as opposed to ~200 km under the Great Plains and ~135 km under the Colorado Plateau. A high velocity signature in the upper mantle is twice as wide as the surface exposure of the rift.

The onset of rifting and rates of extension have been well studied in the major basins of the rift in central New Mexico and southern Colorado (e.g. Chapin and Cather, 1994; Brister and Gries, 1994; Lozinsky, 1994; Lewis and Baldridge, 1994; Cather et al., 1994; Miggins et al., 2002). Geochronology on volcanic rocks interbedded with synrift sediments and uplifted on rift flanks suggests initial basin development and sedimentation in the late Oligocene with the onset of rifting broadly similar from at least New Mexico to the San Luis Basin. The sedimentary record in the southern basins suggests an episode of rapid extension and the development of significant topographic relief along rift flanks in Miocene time (Chapin and Cather, 1994; Cather et al., 1994; Ingersoll, 2001; Miggins et al., 2002). By the close of the Miocene, extension had slowed again and incision replaced aggradation in both the rift basins and off the rift flanks (Chapin and Cather, 1994). At approximately the time of rift initiation, volcanism in the region shifted from intermediate to bimodal (Lipman and Mehnert, 1975).

The Gore Range and adjacent Blue River Valley of central Colorado (Figure 3) represent one of the northernmost fault-related manifestations of the Rio Grande Rift system. The Blue River Valley is a 5-9 km wide half graben bounded by north-trending basement cored uplifts that typify the southern Rockies. The valley is floored by Mesozoic sedimentary deposits and contains a limited quantity of sandstones, gravels and volcanics that are as old as Oligocene. Several east-dipping normal faults cut and offset the Mesozoic deposits within the Blue River Valley (Kellogg, 1999).

The Blue River normal fault separates the valley from the Gore Range and accommodates a minimum vertical displacement of 1.4 km, creating 1.4 km relief in the entirely crystalline southern half of the range (Figure 4a). A cross fault separates the

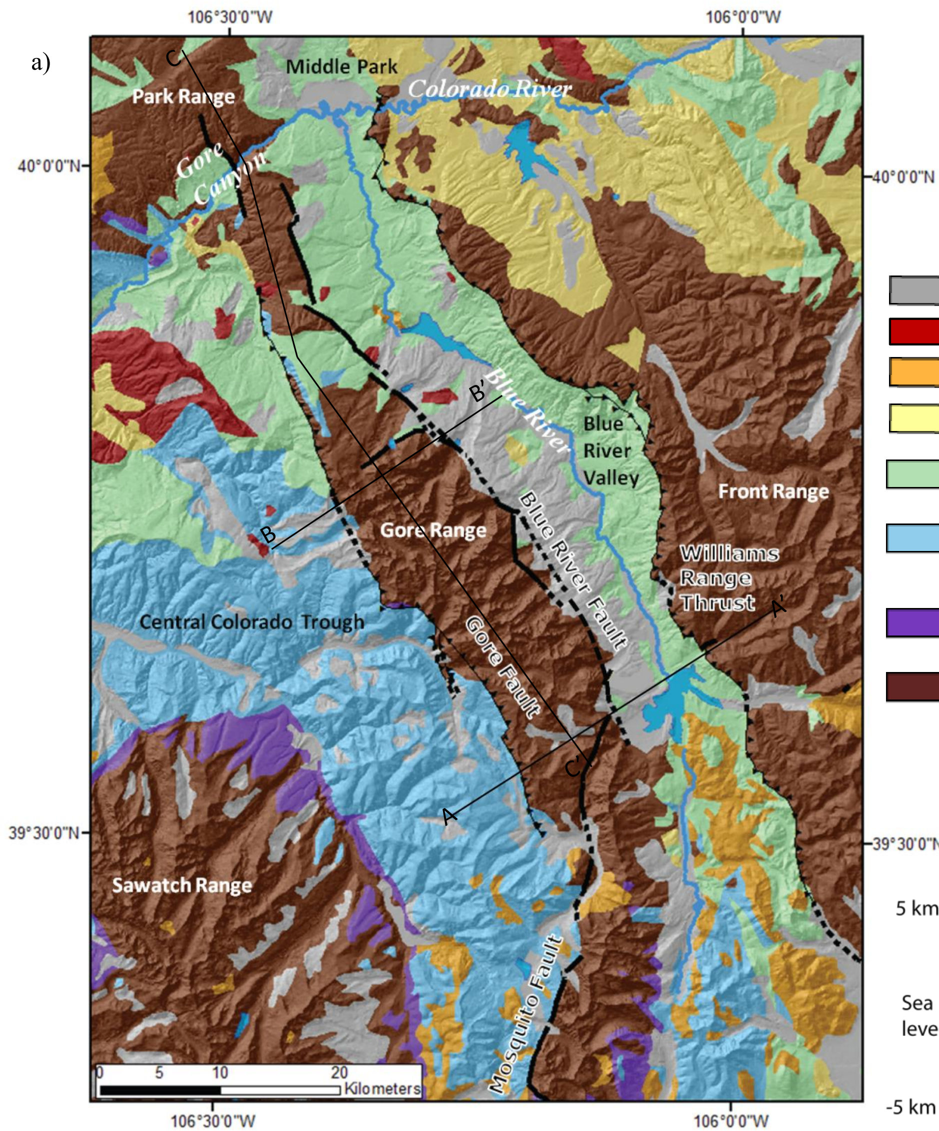

Figure 3: a) Geologic map of the Gore Range, Blue River Valley, and adjacent regions. b) Schematic cross section through the Gore Range, Blue River Valley, and western Front Range, modified from Kellogg et al. (2004), section line A-A' on a). Lines B-B' and C-C' delineate locations of topographic profiles in Figure 4.
Geologic map from Green, 1992.

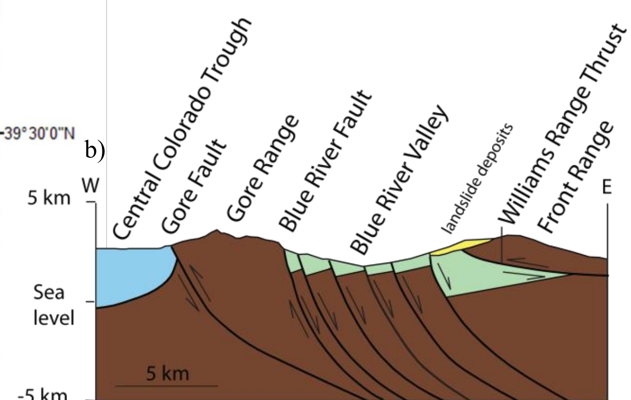

southern from the northern Gores (Naeser et al., 2002). The rolling hills north of the cross fault have a maximum relief of 700 m, and in most places no greater than 200 m (Fig 4b). This section of the range retains a partial cover of Mesozoic sedimentary and Mid-Tertiary volcanic rocks. The high angle Gore reverse fault bounds the western edge of the Gore Range and has been interpreted to sole at depth into the Blue River fault; it may be the surface on which extension in the region is accommodated (Kellogg et al., 2004). On the eastern side of the Blue River Valley, the Williams Range Thrust separates the valley from the crystalline rocks of the Front Range.

The Colorado River flows through Gore Canyon in the northern Gores, adding another 500 m to the vertical bedrock relief (Figure 4b). North of the confluence of the Blue and Colorado Rivers is the Middle Park basin, similar to the Blue River Valley in that it is floored by Mesozoic sedimentary fill at its western boundary with the basement cored Park Range. Further north, North Park and the Saratoga Valley of Wyoming have also been interpreted as Rio Grande Rift basins (Tweto, 1979).

The Proterozoic basement of the Blue River Valley and surrounding uplifts is largely a metamorphic complex variously known as the Idaho Springs Formation, Black Canyon Schist, and the Rocky Mountain Gneiss Complex. In the southern Gore Range the rock is a heavily migmatized biotite gneiss; metamorphic grade decreases to the north where the biotite gneiss is predominately non-migmatized (Kellogg, unpub.). This basement unit was originally deposited as continental margin and backarc clastic marine sediments and volcanics on the southern margin of the Wyoming protocontinent at approximately 1.78 Ga (Tweto, 1987; Fisher and Fisher, 2004) and was sutured to the Wyoming craton between 1.78 and 1.74 Ga (Chamberlain, 1998). During this event the rocks were

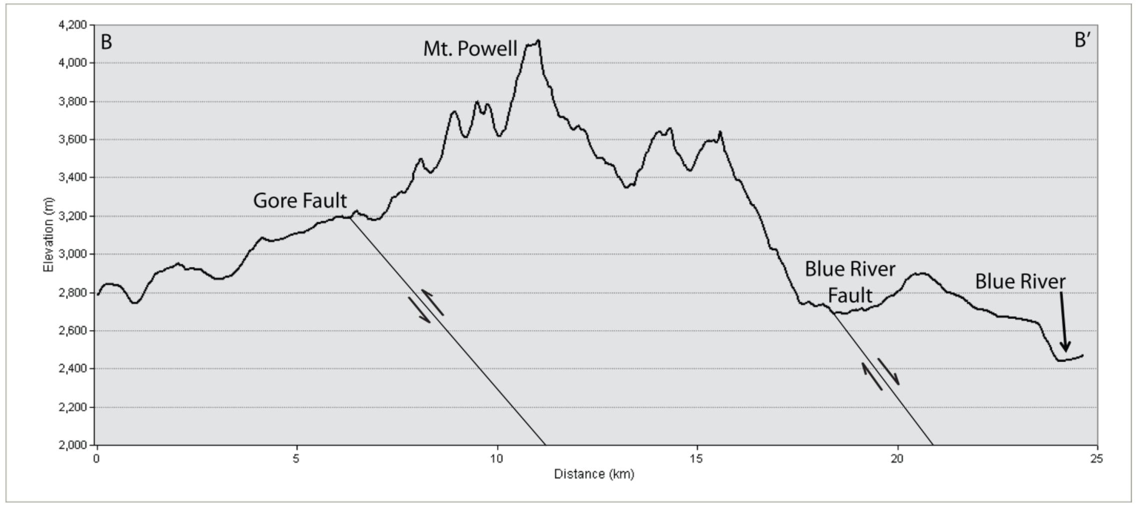

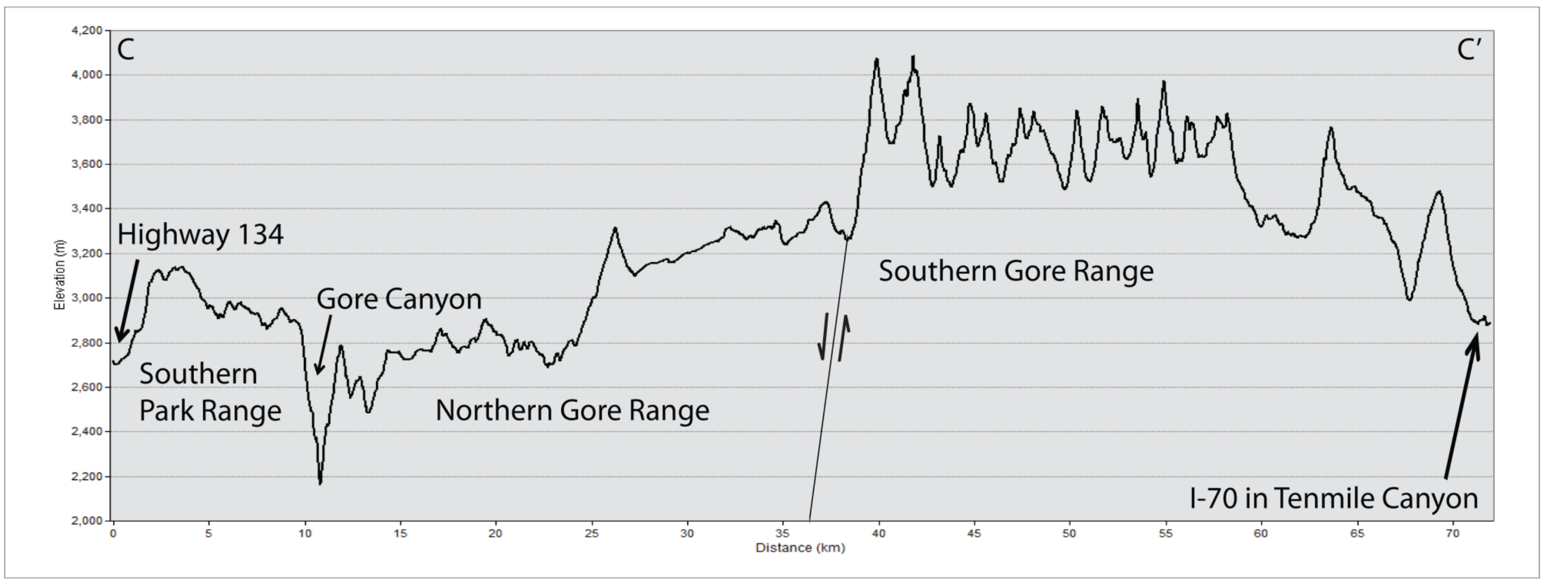

Figure 4: Topographic profiles a) from SW to NE across the southern Gore Range, and b) from NW to SE along the crest of the Gore Range. Locations of profiles are shown in by section lines B-B' and C-C' in Figure 3.

metamorphosed to upper amphibolite grade with peak metamorphism and local anatexis occurring at 1.7 Ga (Kellogg et al., 2003). The Rocky Mountain Gneiss Complex is intruded by 1.7 Ga batholiths of the Routt Plutonic Suite, represented in the Gore Range by the extensive Cross Creek batholith (Tweto, 1987).

The distribution and thicknesses of Paleozoic strata in central Colorado were influenced significantly by a deformation event in late Paleozoic time. Two unconformable relationships with the basement constrain this portion of the region's geologic history. First, marine units of the Cambrian Sawatch Quartzite nonconformably overlie the crystalline basement of the Tenmile Range just south of the high Gores and indicate erosional unroofing prior to Cambrian deposition. The overlying Ordovician Manitou Limestone, Devonian Chaffee Formation, Mississippian Leadville Limestone and Mid-Pennsylvanian Belden Formation indicate that the region remained near sea level during most of early and middle Paleozoic time (Wallace et al., 2003). Although these Paleozoic units are preserved at the southern tip of the Upper Blue River Valley, they are absent everywhere else in the field area. The second important unconformity occurs in the northern Gore Range. Here, the basement is nonconformably overlain by redbeds of the Permian to Lower Triassic State Bridge Formation, indicating erosional removal of the early and middle Paleozoic sequence prior to renewed deposition in the Permian. West of the Gore Range in the Central Colorado Trough, the State Bridge formation sits conformably above the almost 3,000 m thick Mid-Pennsylvanian to Permian alluvial fan and fluvial Minturn and Maroon Formations, both of which thin towards the Gore fault (Kellogg, unpub.).

The erosion of lower Paleozoic units from the Gore Range coeval with deposition of the thick upper Paleozoic sequence to the west reflects the development of the Ancestral Rocky Mountains during the Mid-Pennsylvanian. The Gore fault marked the western boundary of the Ancestral Front Range and may also have been active prior to this time (Kellogg 1999; Kellogg et al., 2003). The low-lying Central Colorado Trough formed as a flexural basin between the Ancestral Front Range and the basement-cored uplift of Uncompaghria to the west (Hoy and Ridgway, 2002), providing accommodation space for the deposition of the Minturn and the Maroon.

The later Mesozoic sedimentary sequence in the region commences with the Jurassic Morrison Formation and Lower Cretaceous Dakota Group, reflecting a return of the region to near sea level. The Morrison and Dakota are the youngest units preserved in the sedimentary section on the northern Gores. In the Blue River Valley, this same sequence is overlain by thousands of meters of marine shales of the Benton Group, Niobrara Formation, and Pierre Shale. These strata mark the advance of the Cretaceous Interior Seaway over the region and its fluctuations throughout Cretaceous time. The youngest ammonite zone in the Pierre Shale is dated at 69 Ma and marks the retreat of the sea from Colorado (Obradovich, 1993).

Several sedimentary units and a Mid- to Late Eocene unconformity constrain the Late Cretaceous and younger tectonic history of the region. The Upper Cretaceous to Paleocene Middle Park Formation is present at the northeastern end of the Blue River Valley and in the Middle Park basin. It consists of volcanic and coarse sedimentary units containing clasts shed from across the Williams Range Thrust (Kellogg, unpub.) and reflects the initiation of crustal shortening and development of relief associated with the

Laramide orogeny in the Late Cretaceous. About 9 km of horizontal shortening was accommodated by the low-angle Williams Range Thrust (Erslev et al., 1999) with additional shortening in the field area along the Gore fault (Kellogg, 2003). In basins on the eastern side of the Front Range the youngest synorogenic Laramide-age strata are overlain by the 37 Ma Wall Mountain Tuff (Raynolds, 2007; Kelley, 2002), this was deposited on a low relief erosional surface that truncates Laramide structural features (Epis and Chapin, 1975). The presence of this surface and the overlying Wall Mountain Tuff suggest that Laramide deformation ceased in central Colorado by the mid-Eocene (Dickinson et al., 1988).

In the Middle Park basin the 245 m thick latest Oligocene to Miocene Troublesome Formation unconformably overlies the Middle Park Formation. The Troublesome contains a basal conglomerate with upper tuffaceous siltstones and sandstones locally interlayered with basalt flows. This unit is coeval with similar units elsewhere in Colorado, including the Browns Park Formation west of the Park Range, the North Park Formation, and the Arikaree and Ogallala Formations on the High Plains (Izett, 1975). The renewed deposition in the region during the Miocene may reflect regional uplift expressed along the flanks of the Rio Grande Rift (e.g. Izett, 1975; Eaton, 1986; Raynolds et al., 2007).

A 500 m thick sedimentary section (Tweto, 1970; Kellogg, unpub.) is preserved in a fault block in the Blue River Valley and imposes key constraints on the Tertiary tectonic and geomorphic history of the Gore Range. A welded tuff directly overlying the basal conglomerate in the Blue River Valley section has been dated at 26.9 ± 0.06 Ma (Naeser et al., 2002) and imposes a minimum age for the initiation of rifting in the study area. A 23.6 ± 0.6 Ma trachyandesite flow near the top of the section and flows of a similar age overlying outcrops of the Morrison, Dakota and Pierre Shale further north in the valley indicate that these Mesozoic units were at the surface at 24 Ma and that there has been relatively little net erosion in the Blue River Valley since that time. Other late Cenozoic igneous activity in the Blue River Valley and Gore Range includes a 31.5 Ma intrusive trachyte complex at Green Mountain (Naeser et al., 2002) and undated basalt flows on the Morrison Formation and crystalline basement in the northern Gores.

During the Quaternary much of the trace of the Blue River fault was covered by glacial deposits (Kellogg et al., 2004). Most movement along the Blue River fault is thought to predate these deposits (West, 1978) but small fault scarps cut till that has been interpreted as Bull Lake age, indicating that faulting may have continued into the mid-Pleistocene (Kellogg et al., 2002).

The Blue and Colorado Rivers drain the Blue River Valley and Middle Park. After flowing westward across the Mesozoic sediments of the western Middle Park valley floor, the Colorado River incises Gore Canyon for a 5 km stretch through the Rocky Mountain Gneiss Complex before emerging on the western side of the Gore Range. A steep knickzone in the Colorado River is currently located within the canyon (Karlstrom et al., 2008).

3. Apatite (U-Th)/He thermochronometry

Low temperature thermochronometry is a powerful technique that can aid in deciphering unroofing and uplift histories. Apatite (U-Th)/He thermochronometry is based on the radioactive decay of trace quantities of uranium and thorium in apatite grains. The isotopes ^{238}U, ^{235}U and ^{232}Th decay to produce ^{4}He. As a result, the amount of parent and daughter elements present in apatite grains can be used to determine the amount of time that has passed since an apatite-bearing rock cooled through the closure temperature using the equation: $^{4}He_{all}$ = 8 [137.88 / (1 + 137.88)] C_U ($e^{\lambda 238t}$ – 1) + 7 [1/(1+137.88)] C_U ($e^{\lambda 235t}$ - 1) + 6C_{Th}($e^{\lambda 232t}$ – 1)] (Harrison and Zeitler, 2005). In this equation C_U and C_{Th} are the concentrations of uranium and thorium, λ is the decay constant of each of the specified isotopes, and t is time. (U-Th)/He ages must also be corrected for He alpha recoil. He particles produced by decay within the outer 20 μm of apatite grains may be ejected from the grain. By measuring the size and shape of grains it is possible to correct for the proportion of a mineral's ^{4}He that has been lost by ejection (Farley et al., 1996).

As a noble gas, He diffuses readily out of apatite grains at temperatures found in most of the earth's crust but is partially retained at temperatures below ~70-80 °C, and completely retained at temperatures below ~30-40 °C (Wolf et al., 1996; Harrison and Zeitler, 2005). For simple monotonic cooling histories, apatite (U-Th)/He dates are commonly interpreted to record the time of cooling through the ~70 °C isotherm (Farley, 2000). By assuming a geothermal gradient it is possible to derive an exhumation history for a sample from its cooling history. The 70 °C isotherm is usually 1.5-3 km below the surface. Although the closure temperature is sometimes expressed as a single temperature, the transition from complete He loss to complete He retention does not occur instantaneously. Instead, a rock will pass through a partial retention zone (PRZ) on its path to the surface (Figure 5). In this zone the sample experiences a growing rate of He retention. The PRZ in apatite encompasses temperatures from ~40-85 °C (Dunai, 2005). A rock that has spent a prolonged period in the PRZ will produce cooling dates that do not correspond to a specific isotherm.

Apatite fission-track is another commonly used low-temperature thermochronometer and is typically sensitive to somewhat higher temperatures than the apatite (U-Th)/He technique. This method is based on the spontaneous fission of uranium in apatite grains and is commonly used to infer cooling histories from ~120-60 °C, with the closure temperature commonly given as 110 °C (Donelick et al., 2005), or about 3-5 km depth.

4. Previous thermochronometry in the southern Rocky Mountains

Extensive AFT datasets have been acquired in the Rio Grande Rift and southern Rocky Mountains since the 1960's (Figure 2), revealing several distinct patterns. At the highest elevations such as the top of Pikes Peak and Mount Evans in the Colorado Front Range, Mid-Mesozoic and older fission-track dates are preserved (Bryant and Naeser, 1980; Kelley and Chapin, 2004). These dates have been interpreted to reflect rocks that were at near-surface conditions prior to the Laramide orogeny. Much of the Colorado Rockies and selected uplifts in northern and central New Mexico preserve Late Cretaceous and Early Tertiary dates, reflecting passage through the ~110 °C isotherm during uplift and exhumation caused by latest Cretaceous and Early Tertiary mountain

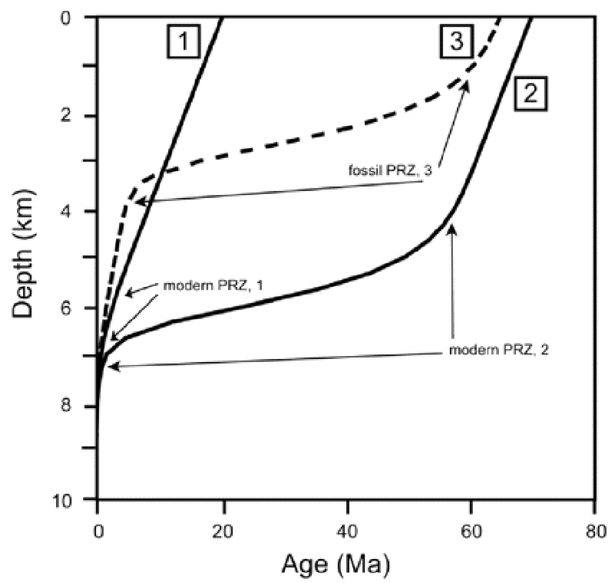

Figure 5: Schematic depiction of the concept of the apatite helium partial retention zone (PRZ), with the lines representing the predicted relationships between depth and apatite (U-Th)/He date for three different exhumational histories. Line 1 represents continuous erosion and exhumation and line 2 represents a period of erosion and exhumation followed by a period of no tectonic activity. Line 3 represents line 2 with an additional period of exhumation. From Harrison and Zeitler, 2005.

building (Bryant and Naeser, 1980; Kelley et al., 1992; Kelley and Chapin, 2004; Kelley, 2005). The boundary between pre-Laramide (older than ~75 Ma) and Laramide ages (~75-45 Ma) has been identified as a valuable structural datum in the crystalline rocks of the Colorado Rocky Mountains (Kelley and Chapin, 2004.) Rocks with Mid-Tertiary or younger AFT cooling dates are not common in Colorado. Instead, cooling dates of this age are almost entirely found in ranges bounding Rio Grande Rift basins in the southern and central parts of the state (Lindsey et al., 1986; Kelley et al., 1992; House et al., 2003; Kelley and Chapin, 2004). The same pattern has been found in the rift flank uplifts of New Mexico, where cooling ages young from the tops of ranges towards the basin-bounding faults.

(U-Th)/He data is sparse in the central and southern Rocky Mountain. One (U-Th)/He study has been performed in the central Rockies, in the Bighorn Mountains of Wyoming. These samples yielded Devonian to early Paleocene dates (Crowley et al., 2002). The only published (U-Th)/He dataset from the Rio Grande Rift is from the Sandia Mountains outside of Albuquerque, New Mexico. These dates ranged from 12.9 ± 0.9 to 18.5 ± 1.3 Ma (House et al., 2003). No (U-Th)/He dataset has been published for anywhere in Colorado.

5. Approach and methods

Eleven out of the fifteen samples in this study are from mineral separates kindly shared by C. Naeser. These separates were previously dated via AFT thermochronology (Naeser et al., 2002; Appendix 1). Other samples were collected during fall 2008 and the summer and fall of 2009. Much of the fieldwork was targeted at collecting samples that would complement the separates shared by C. Naeser. The eastern edge of the range was the focus during these field seasons because that area was likely to yield the youngest dates. I collected low elevation samples from six different drainages along the eastern Gore Range, from Cataract Creek to South Willow Creek, and corresponding high elevation samples in three of those drainages. I also collected samples from three drainages in the Tenmile Range – Miners Creek near Frisco, Ski Hill Creek near Breckenridge, and McCullough Gulch below Quandary Peak – in order to examine the relationship between the Gore and Tenmile Ranges. Processing these samples revealed that the Cross Creek batholith is an excellent source of datable apatite grains, but that the migmatitic biotite gneiss contained few to no apatite grains of sufficient quality. Granitic gneiss and plagioclase-hornblende gneiss near the town of Frisco did yield suitable apatites.

Mineral separation was accomplished using standard crushing, wilfley table, heavy liquid, and magnetic separation techniques. Single crystals of apatite were selected based on morphology, clarity, and lack of inclusions using a binocular microscope with crossed polars. Prior to analysis, grains were photographed, grain dimensions were measured, and the apatites were individually placed in Pt packets.

All data were acquired at the California Institute of Technology. Apatite grains were laser heated to 1065 °C for eight minutes (House et al., 2000). Extracted He gas was spiked with ^{3}He, purified using cryogenic and gettering methods, and analyzed on a quadrupole mass spectrometer. The degassed apatites were retrieved, spiked with a ^{235}U-^{230}Th-^{51}V tracer, dissolved in HNO_3 at ~90 °C for 1 hour, and analyzed on an Agilent ICP-MS at the California Institute of Technology. The apatite mass was computed from the apatite Ca concentration using ^{51}V as an elemental spike. This Ca-based mass was used to calculate the apatite U and Th concentrations. Fragments of the Durango apatite standard were analyzed by the same procedures with the batch of unknowns. A hexagonal prism morphology was used for the alpha-ejection correction and applied to all crystals (Farley et al., 1996).

All analytical results are listed in Table 1. Analytical uncertainties for individual analyses are based on the propagated error from the U, Th, and He analyses and grain length measurements. Sample results discussed in the text below and plotted in all figures are reported as the sample mean and the 1σ sample standard deviation of the mean. In September of 2009, five samples were prepared and sent for $^{4}He/^{3}He$ analysis. The $^{4}He/^{3}He$ thermochronometer can trace a cooling history to as low as 30 °C by using step heating to ascertain the distribution of ^{4}He within an apatite crystal (Shuster and Farley, 2005). Results have not been received at this time.

Some factors can complicate the interpretation of (U-Th)/He dates. Both large-scale topography and erosion across active faults can cause isotherms to curve (Ehlers, 2005). If samples are cooled and then reheated due to events like magmatism or reburial, the cooling ages may be partially, but not entirely, reset (Reiners, 2009). Recent work has shown that a lower apatite He diffusivity can be positively correlated with the amount of He present in the crystal; the radioactive decay that produces the He also damages the crystal structure and causes the effective closure temperature to increase (Flowers et al., 2009). The flow of groundwater in the shallow crust can lower isotherms over the range crest and raise isotherms around the boundary between the range and the basin (Ehlers, 2005). However, a recent study involving both borehole temperature profiles and noble

Table 1: Apatite (U-Th)/He data from the southern Gore Range

	Mass (μg)	Radius (μm)	Length (μm)	U (ppm)	Th (ppm)	(eU) (ppm)	^{4}He (nmol/g)	Ft	Raw date (Ma)	Corr date (Ma)	Error (Ma)	Mean date (Ma)	1σ std dev (Ma)
L09-BL4, Cross Creek granite, 3016 m												**33.1**	**2.6**
a1	8.1	81	196	22.4	4.7	23.5	3.7	0.81	28.1	**34.6**	0.9		
a2	3.9	52	182	24.2	4.0	25.1	3.5	0.73	25.3	**34.3**	1.1		
a3	3.2	52	248	35.3	4.9	36.4	5.4	0.75	26.6	**35.4**	1.1		
a4	4.3	55	258	42.6	14.8	46.1	6.2	0.76	24.5	**32.2**	0.9		
a5	2.0	40	150	15.7	1.9	16.2	1.8	0.67	19.6	**28.9**	1.3		
L09-H92, hornblende-plagioclase gneiss, 2853 m												**31.0**	**2.3**
a1	13.4	94	287	91.7	45.2	102.3	15.2	0.84	27.3	**32.3**	0.7		
a2	5.0	70	176	123.6	77.1	141.7	20.5	0.78	26.5	**33.9**	0.8		
a3	3.6	61	143	49.1	50.2	60.9	7.2	0.74	21.6	**29.0**	0.8		
a4	2.8	55	158	51.7	24.5	57.5	6.6	0.73	20.9	**28.5**	0.8		
a5	2.8	51	162	57.3	68.2	73.4	9.5	0.72	23.7	**32.9**	1.0		
a6	1.9	50	125	29.2	26.9	35.5	4.0	0.70	20.7	**29.5**	1.0		
MP97-289, Cross Creek granite, 3011 m												**15.1**	**3.7**
a3	1.2	35	113	23.1	12.8	26.1	1.7	0.61	11.9	**19.3**	0.9		
a4	1.3	34	132	21.3	8.0	23.2	1.0	0.61	7.6	**12.3**	0.7		
a6	0.6	30	109	43.0	18.2	47.3	2.0	0.56	7.7	**13.6**	0.8		
GRWL1, mafic inclusion in Cross Creek granite, 3911 m												**18.6**	**1.4**
a1	3.0	50	179	75.7	7.9	77.6	6.3	0.73	14.9	**20.5**	0.6		
a2	2.8	53	172	76.2	24.2	81.9	6.3	0.73	14.0	**19.0**	0.5		
a3	1.9	37	220	32.2	9.1	34.4	2.1	0.66	11.3	**17.0**	0.7		
a4	2.0	43	164	27.8	7.6	29.6	2.1	0.69	12.9	**18.7**	0.7		
a6	0.9	33	137	30.3	2.1	30.8	1.8	0.61	10.9	**17.5**	0.9		
GRWL2, migmatitic inclusion in Cross Creek granite, 3755 m												**18.8**	**2.9**
a1	7.3	72	339	29.1	0.2	29.1	2.8	0.81	17.7	**21.7**	0.6		
a2	3.4	48	182	97.5	1.0	97.7	6.8	0.72	12.7	**17.6**	0.5		
a3	2.8	46	219	62.7	1.4	63.0	4.9	0.72	14.2	**19.7**	0.6		
a4	3.1	54	177	14.2	0.9	14.4	0.8	0.74	10.5	**14.0**	0.6		
a5	2.7	53	139	127.1	0.5	127.2	10.9	0.72	15.7	**21.6**	0.6		
a6	2.3	52	119	99.8	0.4	99.9	7.0	0.71	12.8	**18.0**	0.5		
GRWL3, Cross Creek granite, 3603 m												**17.1**	**1.6**
a1	9.4	80	241	28.1	0.3	28.1	2.4	0.82	15.6	**19.0**	0.5		
a2	4.5	50	238	15.6	0.9	15.8	1.1	0.74	13.0	**17.6**	0.6		
a3	4.6	57	218	11.1	0.4	11.2	0.8	0.76	12.4	**16.2**	0.6		
a4	6.7	71	277	8.2	0.6	8.4	0.6	0.81	12.6	**15.6**	0.6		
a5	4.7	62	301	29.6	0.4	29.7	2.4	0.79	14.5	**18.4**	0.5		
a6	3.2	67	216	11.3	0.4	11.4	0.7	0.79	11.6	**14.6**	0.6		
GRWL8, Cross Creek granite, 3230 m												**11.6**	**2.3**
a1	4.1	53	218	13.3	68.9	29.5	1.6	0.73	10.0	**13.6**	0.4		
a2	3.3	44	176	20.4	34.8	28.5	1.5	0.69	9.8	**14.2**	0.5		
a3	3.1	52	156	9.5	61.2	23.8	0.9	0.71	6.7	**9.4**	0.3		
a4	2.6	48	146	13.1	32.6	20.8	0.9	0.69	7.9	**11.4**	0.5		
a5	2.0	47	121	5.0	33.4	12.9	0.4	0.67	6.2	**9.3**	0.5		
L09-BL3, Cross Creek granite, 3201 m												**15.2**	**3.7**
a1	23.8	101	366	15.8	0.9	16.0	1.1	0.86	12.5	**14.6**	0.3		
a2	4.4	64	173	17.7	2.3	18.2	1.2	0.77	11.9	**15.5**	0.5		
a3	3.2	58	240	9.5	0.3	9.5	0.4	0.77	8.0	**10.4**	0.5		
a4	4.6	52	297	10.4	0.7	10.6	0.5	0.75	9.2	**12.1**	0.5		
a5	3.1	47	195	15.1	0.3	15.1	1.1	0.72	13.3	**18.4**	0.8		
a6	2.3	40	158	16.9	0.2	16.9	1.3	0.67	13.6	**20.1**	0.9		
L09-BL2, Cross Creek granite, 3102 m												**10.2**	**0.9**
a1	5.8	71	183	21.7	2.0	22.2	1.0	0.79	8.5	**10.8**	0.3		
a2	3.2	57	150	20.2	3.9	21.1	0.9	0.74	8.1	**10.9**	0.4		
a3	4.3	59	184	11.6	1.8	12.0	0.5	0.76	7.2	**9.4**	0.4		
a4	2.5	54	133	26.7	5.1	27.9	1.1	0.72	7.4	**10.1**	0.4		
a5	1.3	43	124	11.2	2.1	11.7	0.5	0.67	7.7	**11.4**	0.9		
a6	3.2	70	140	12.5	1.9	13.0	0.5	0.77	6.9	**8.9**	0.4		

	Mass (μg)	Radius (μm)	Length (μm)	U (ppm)	Th (ppm)	(eU) (ppm)	^{4}He (nmol/g)	Ft	Raw date (Ma)	Corr date (Ma)	Error (Ma)	Mean Date (Ma)	1σ std dev (Ma)
GRF1, granitic gneiss, 2791 m												**6.9**	**2.8**
a1	10.2	72	192	8.1	0.2	8.2	0.2	0.79	4.5	**5.7**	0.2		
a2	6.8	69	198	6.0	0.1	6.0	0.1	0.79	3.9	**4.9**	0.3		
a3	3.8	44	146	5.1	0.3	5.2	0.2	0.69	6.9	**10.0**	0.6		
MP97-284, Cross Creek granite, 4139 m												**41.8**	**5.3**
a1	4.0	47	276	32.6	0.3	32.7	4.9	0.73	27.3	**37.2**	1.1		
a2	4.4	57	174	55.9	1.1	56.2	9.9	0.75	32.3	**43.0**	1.2		
a3	4.7	63	165	53.0	1.0	53.3	9.2	0.76	31.6	**41.3**	1.1		
a4	1.9	40	155	152.4	1.3	152.8	28.8	0.67	34.5	**51.4**	1.6		
a5	1.2	38	116	25.5	0.5	25.6	3.3	0.64	23.7	**36.8**	1.6		
a6	1.8	34	181	133.5	1.4	133.8	19.4	0.64	26.6	**41.5**	1.4		
MP97-287, Cross Creek granite, 3658 m												**37.7**	**2.9**
a1	3.0	43	194	58.1	0.4	58.2	8.3	0.70	26.1	**37.4**	1.2		
a2	1.6	40	163	91.9	2.0	92.3	13.4	0.67	26.5	**39.1**	1.3		
a3	1.6	37	163	68.5	0.1	68.6	9.3	0.65	24.8	**37.8**	1.3		
a4	1.7	36	274	88.6	2.5	89.1	11.0	0.66	22.5	**33.8**	1.1		
a5	2.2	32	182	60.0	1.6	60.4	8.6	0.62	26.1	**42.0**	1.5		
a6	1.4	42	166	61.3	0.8	61.5	8.2	0.68	24.2	**35.2**	1.2		
GRVP14, Cross Creek batholith tonalite, 3716 m												**40.4**	**4.3**
a4	0.7	30	176	32.6	24.7	38.4	4.8	0.59	22.5	**37.7**	1.9		
a5	2.0	42	255	38.9	27.0	45.2	6.6	0.69	26.7	**38.2**	1.3		
a6	2.2	47	218	45.4	28.3	52.0	9.4	0.72	32.8	**45.4**	1.4		
GRWL12, Cross Creek batholith tonalite, 3746 m												**29.8**	**3.0**
a1	2.1	45	165	40.3	32.8	48.0	5.0	0.69	18.9	**27.1**	0.9		
a2	2.3	44	206	35.2	45.0	45.8	5.7	0.70	22.6	**32.2**	1.1		
a3	1.5	39	191	32.4	44.0	42.7	5.2	0.66	21.7	**32.6**	1.2		
a4	1.1	36	179	31.9	32.5	39.5	3.7	0.64	16.7	**25.6**	1.1		
a5	0.7	27	146	40.2	36.6	48.8	4.4	0.55	16.2	**28.9**	1.5		
a6	1.4	44	142	50.0	63.8	65.0	7.9	0.68	22.0	**32.3**	1.1		
GRWL10, Cross Creek granite, 3032 m												**31.1**	**2.3**
a1	10.6	79	252	56.4	0.9	56.6	8.4	0.82	27.0	**32.9**	0.7		
a2	7.3	71	306	26.5	1.5	26.9	3.6	0.81	24.3	**30.0**	0.8		
a3	6.1	64	187	26.8	0.6	27.0	3.5	0.77	23.5	**30.3**	0.8		
a4	5.5	64	268	26.4	0.6	26.6	3.3	0.79	22.7	**28.7**	0.8		
a5	6.4	65	323	73.4	1.0	73.7	9.5	0.80	23.6	**29.6**	0.7		
a6	6.9	71	185	70.5	0.5	70.6	10.6	0.79	27.6	**34.8**	0.8		

Ft is the alpha ejection correction of Farley et al., 1996.
Error is the 1σ propagated error from the analytical uncertainties on U, Th, and He analyses and grain-length measurement uncertainties.
Sample locations and AFT dates from Naeser et al., 2002, are listed in Appendix 1.

gas measurements of a small watershed in the Colorado Front Range indicated that groundwater in the metamorphic bedrock was only circulating within 200 m of the surface (Manning and Caine, 2007). Given the similarity of the Gore Range and the Front Range in both topography and rock type, this suggests that groundwater flow should not distort geotherms or (U-Th)/He cooling ages in the Gore Range.

6. Results

This study presents apatite (U-Th)/He dates for 78 individual apatite crystals from 15 samples in and around the southern Gore Range (Figure 6). Samples were collected over an elevation span from 2791 to 4139 m on both the eastern and western sides of the southern Gore Range. Thirteen of the samples were from the 1.7 Ga Cross Creek batholith, while two samples were from a granitic gneiss and a plagioclase-hornblende gneiss of similar age. Mean apatite (U-Th)/He dates ranged from 6.9 ± 2.8 to 41.8 ± 5.3 Ma (Figures 6, 7). The results can be subdivided into three groups based on across-strike location in the range and sample dates: 1) eight samples from the eastern Gore Range characterized by Miocene dates, 2) the two samples furthest east of the range crest with Mid-Tertiary dates, and 3) five samples from the western Gore Range characterized by Mid-Tertiary dates.

Of the eight samples in the first group (red outlines on Figures 6, 7*),* six made up a transect on Keller Mountain spanning 3102 to 3911 m in elevation. These samples yielded dates from 18.8 ± 2.9 to 10.2 ± 0.9 Ma. A seventh sample (MP97-289) from 11.5 km northwest of Keller Mountain at an elevation of 3011 m yielded a date of 15.1 ± 3.7 Ma, consistent with results from the Keller Mountain transect. The final sample in this

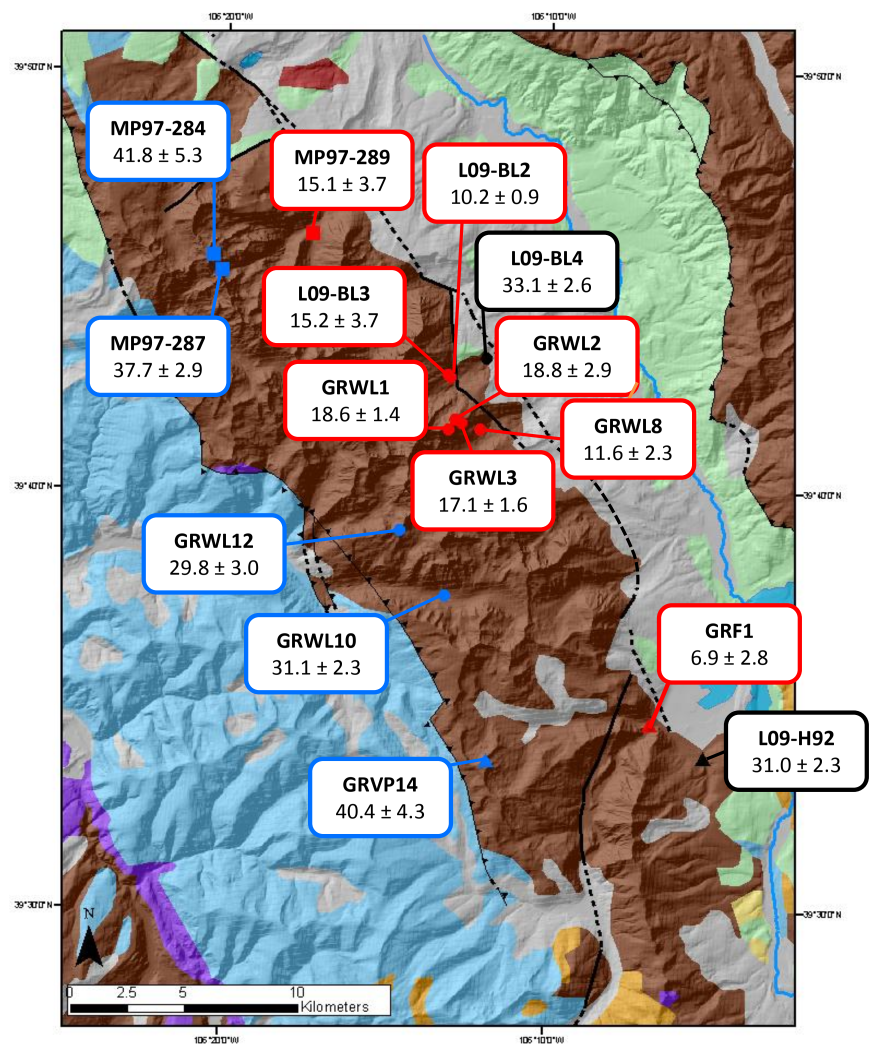

Figure 6: Geologic map of the southern Gore Range showing sample locations and dates. Apatite (U-Th)/He dates are reported as the mean with error as the 1σ sample standard deviation of the mean.

Western samples, mid-Tertiary cooling ages:

- ■ Northern range
- ● Central range
- ▲ Southern range

Eastern samples, Miocene cooling ages:

- ■ Northern range
- ● Central range
- ▲ Southern range

Easternmost samples, mid-Tertiary cooling ages:

- ● Central range
- ▲ Southern range

Figure 7: Age-elevation profile for the southern Gore Range.

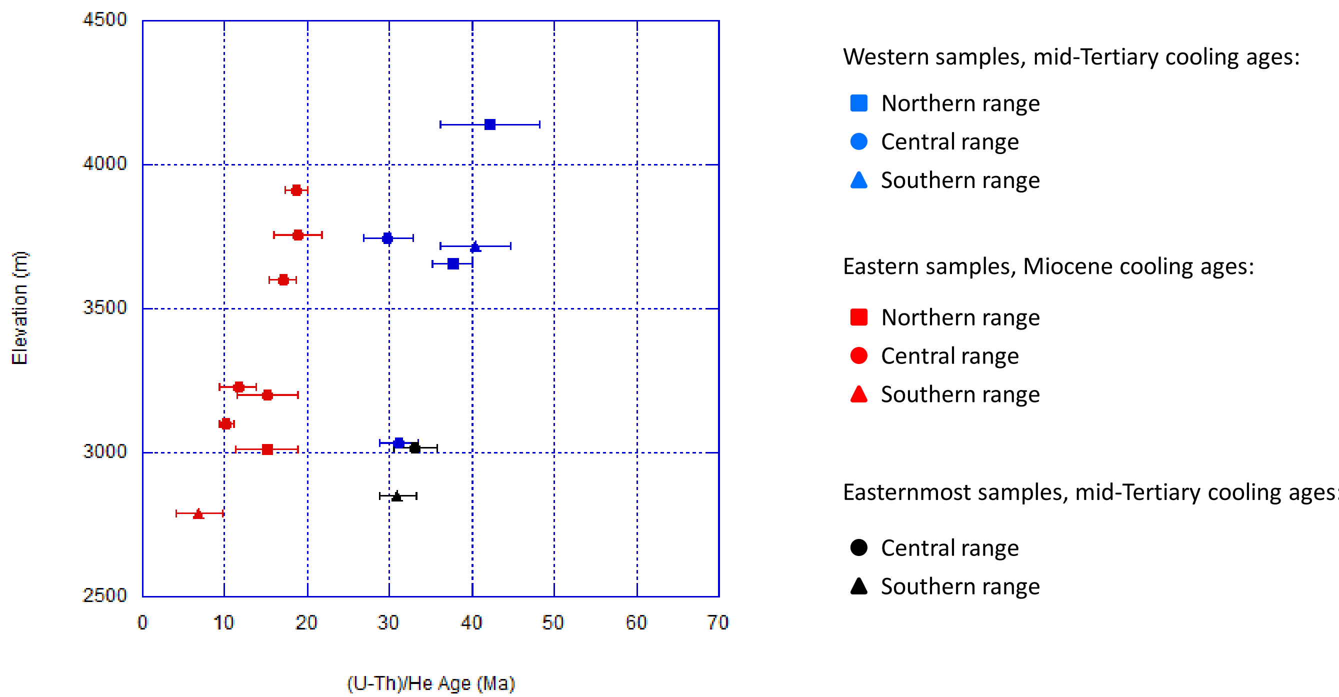

group (GRF1) was collected 16 km southeast of Keller Mountain at the eastern entrance to Tenmile Canyon. This is the lowest elevation sample of our sample suite (2791 m) and yielded the youngest date at 6.9 ± 2.8 Ma.

The two samples in the second group (black outlines, Figures 6, 7) were from localities 16 km apart along the range front. L09-BL4 was collected in the same drainage as the lowest sample in the Keller Mountain transect described above, but 1 km east of that sample and 100 m lower (3016 m). Despite its proximity to samples with Mid- to Late Miocene dates, this sample yielded a significantly older date of 33.1 ± 2.6 Ma. The second sample in this group (L09-H92) was collected from an outcrop on the eastern edge of the Tenmile Range. This sample was also geographically close to a sample with a Late Miocene date – 2.5 km to the southeast of the youngest sample in the dataset and only at a slightly higher elevation (2853 m) – but yielded a Mid-Tertiary date of 31.0 ± 2.3 Ma.

The five samples in the third group (blue outlines, Figures 6, 7) were from three widely spaced locations on the western side of the range. One pair of samples came from Mount Powell, the highest point in the Gore Range and near the boundary with the northern Gores. Sample MP97-284 from the summit of Mount Powell (4139 m) and MP97-289 from ~500 m below the summit yielded dates of 41.8 ± 5.3 Ma and 37.7 ± 2.5 Ma respectively. Another pair of samples (GRWL12 and GRWL10) from the vicinity of the Gore Creek drainage, ~ 17 km to the southeast of Mount Powell, yielded dates of 29.8 ± 3.0 Ma (3746 m) and 31.1 ± 2.3 Ma (3032 m). A single sample (GRVP14) at the southwestern corner of the range at 3716 m yielded a date of 40.4 ± 4.3 Ma.

7. Middle to Late Cenozoic thermal history of the Gore Range

7.1. Structural depth estimates

The age-elevation profile for this dataset (Figure 7) reveals younger dates in the eastern than in the western part of the range, and also shows two eastern sample outliers with older dates. However, the modern age-elevation profile does not directly mimic the age-paleodepth profile in a tilted fault block such as the Gore Range (Figure 8a). The pre-extension paleodepth of rocks currently at the surface in the southern Gore Range cannot be constrained directly because of the lack of sedimentary and volcanic cover in this region. A range of post-extension structural tilts ranging from 5° to 60° were evaluated to reconstruct the relative pre-extension depths of the samples and therefore facilitate interpretation of the cooling history (Figure 8b). The substantial range of tilts is based on work in other flank uplifts of the Rio Grande Rift where tilting is well constrained by sedimentary and volcanic units. The Lemitar Mountains in the central Rio Grande Rift divide the Socorro and La Jencia Basins. This range experienced a maximum tilting since the Late Eocene of 65-75° judging from volcanic units emplaced at that time, with 35-45° of this tilting since 16 Ma based on stratal dips of the Popotosa formation (Cather et al., 1994). Basalt flows preserved in the footwall of the Sangre de Cristo fault bounding the San Luis Basin have been tilted up to 25° since 15 Ma (Miggins et al., 2002).

Tilt reconstructions for the Gore Range demonstrate that at structural tilts of 10°, the highest eastern samples of Miocene age are at an equivalent paleodepth to the lowest western samples of Mid-Tertiary age. Therefore 10° is chosen as the minimum possible structural tilt. Reconstructions with structural tilts above 25° would require very rapid cooling at around 40 Ma, an interpretation that does not correspond to any event known a)

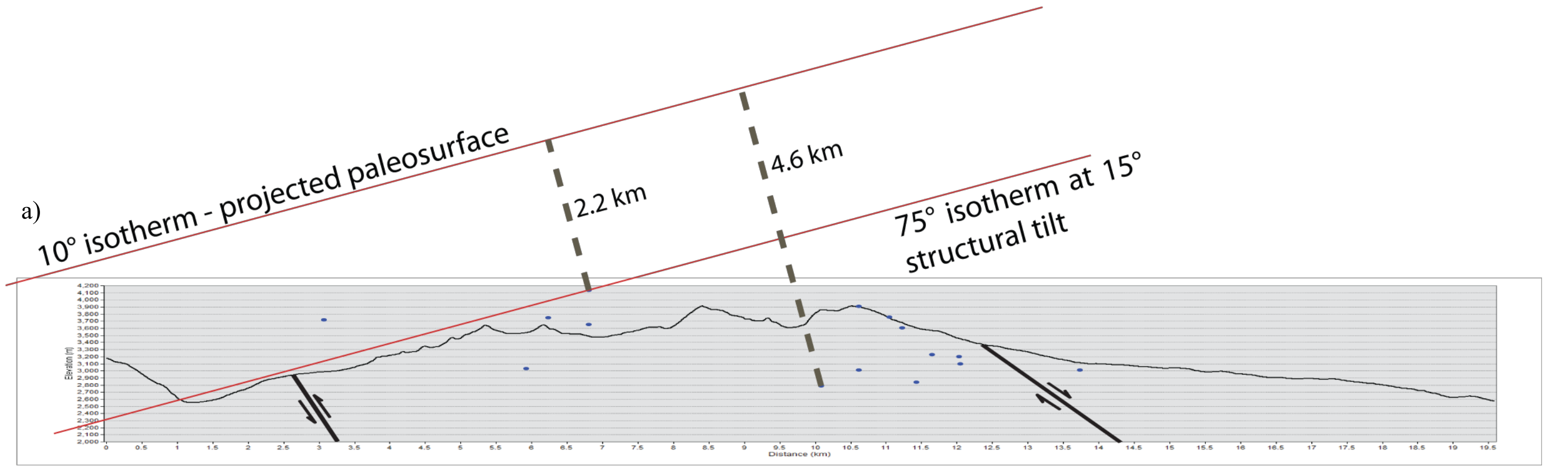

Figure 8: a) Schematic representation of paleodepths in the Gore Range. The age-elevation relationships of samples in the modern Gore Range are not equivalent to pre-extension age-paleodepth relationships. In order to more accurately interpret cooling histories, a range of structural tilts was applied to the tilted fault block. In this figure, samples are plotted on a cross section through the modern Gore Range. Because we cannot precisely constrain the temperature or depth of any sample prior to extension with our current dataset, and because the geothermal gradient may have varied over time, on the graphs in Figure 7b paleodepths are simply represented as elevations relative to sample MP97-284, at 4139 m on the modern Gore Range surface. However, with additional assumptions we can estimate paleodepths in the following manner. For example, if we 1) assume the modern highest sample, MP97-284, was located near the bottom of a He partial retention zone (75 C isotherm) developed in the late Eocene prior to extension, 2) apply a geothermal gradient of 35 C/km, and 3) use a paleosurface temperature of 10 C, then the depth of 75 C isotherm is predicted to be 2.2 km below the surface. All isotherms are then tilted from the horizontal, with the depths of all other samples measured relative to the estimated paleosurface. This exercise is intended to demonstrate the approach for calculating sample paleodepths, but we do not discuss this further in the text because of the current uncertainties in these estimates.
b) Structural tilt reconstructions with results plotted as depth below the modern surface versus age for a range of tilt magnitudes.

b)

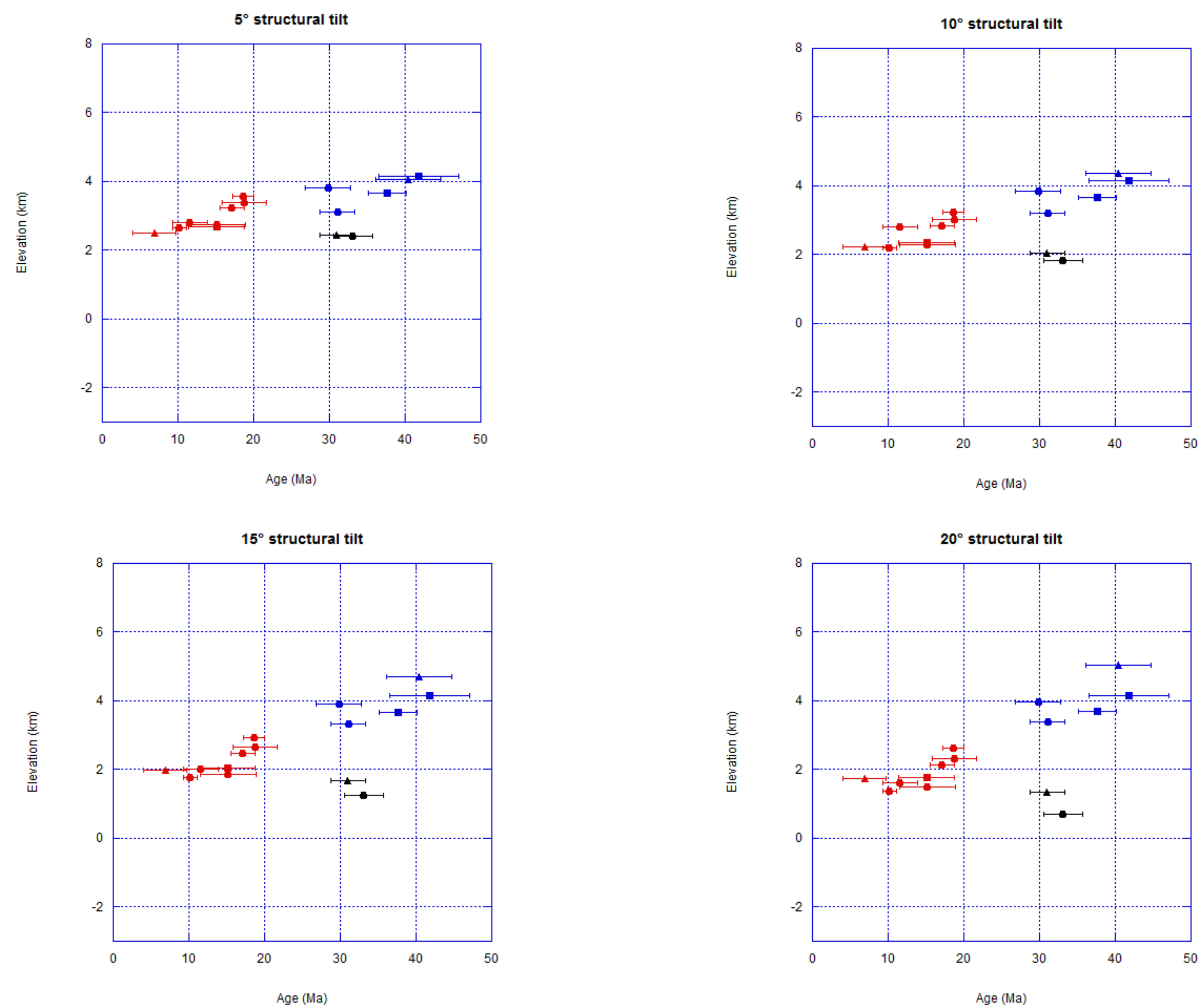

5° structural tilt
10° structural tilt
15° structural tilt
20° structural tilt
Elevation (km)
Age (Ma)
8
6
4
2
0
-2
0
10
20
30
40
50

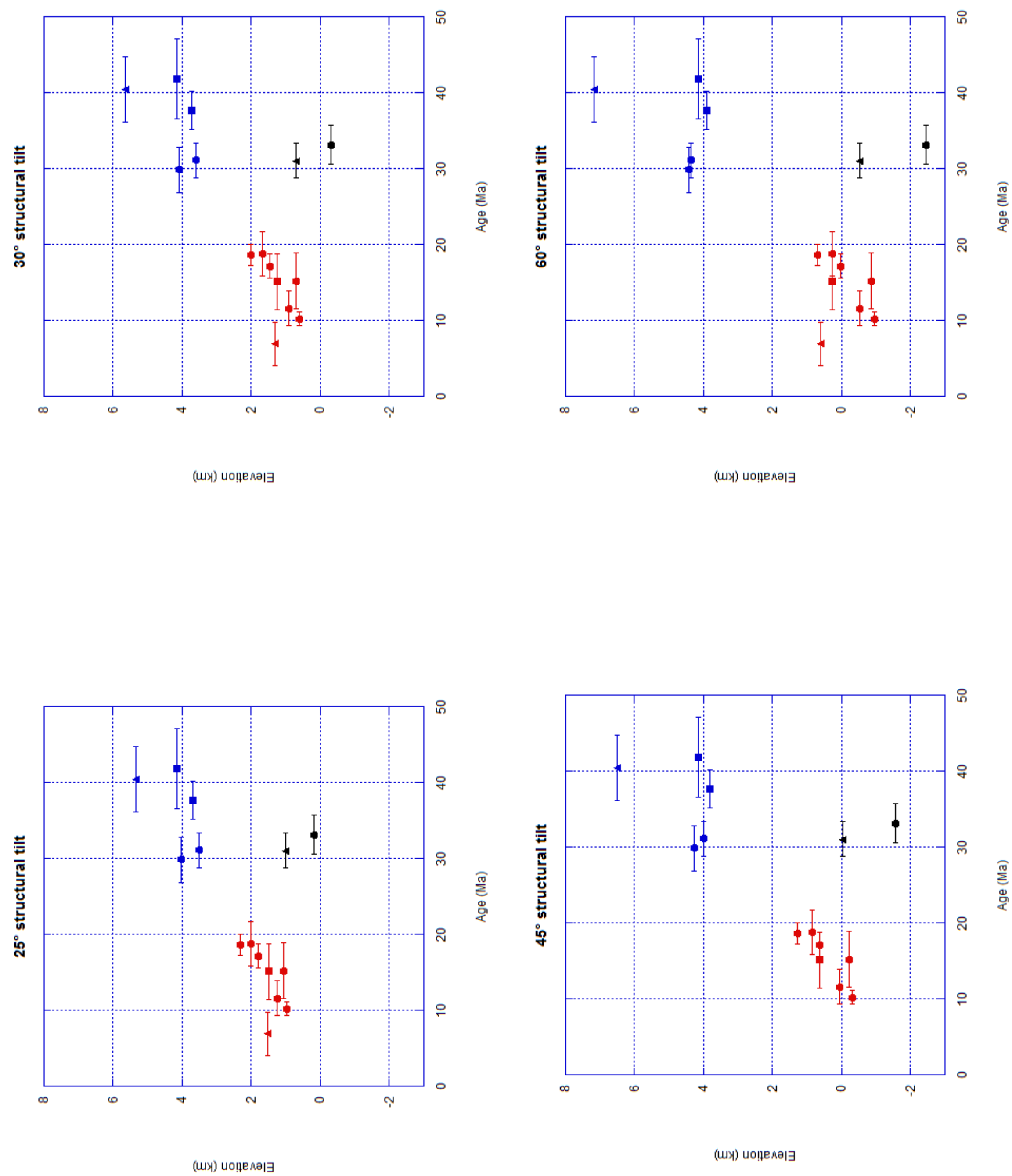

30° structural tilt
60° structural tilt
25° structural tilt
45° structural tilt
Elevation (km)
Age (Ma)

to have occurred in the region (further discussion below). In addition, extension in Rio Grande Rift basins decreases towards the north. South of Socorro, New Mexico, extension was sufficient to cause basement blocks to emerge to the surface and divide the Rio Grande Rift into several pairs of parallel basins similar to those found in the Basin and Range province (Chapin and Cather, 1994). In the northernmost of these areas, the Popotosa Basin of central New Mexico, extension is ~55% (Cather et al., 1994). In the southern Albuquerque Basin extension is estimated at 28%, decreasing to 17% in the northern Albuquerque basin (Russell and Snelson, 1990). Further to the north, the San Luis Basin has experienced only 8-12% extension (Kluth and Schaftenaar, 1994). The continued decrease in graben width in the Upper Arkansas and Blue River Valleys indicates that decreasing extension continues to the north. The amount of tilting in the Gore Range should not approach the 35-45° of stratal tilting in the Lemitar Mountains of the Popotosa Basin, and probably not even the 25° of the Culebra Range bounding the San Luis Basin. For these reasons, reconstructions with structural tilts between 10° and 20° are the favored interpretations.

The interpretation of the cooling history of the Gore Range must take into account four first order features of the age-paleodepth reconstructions. All of these will be discussed in further detail below. First, the youngest apatite (U-Th)/He date in the range provides a minimum estimate of unroofing in that location since the Late Miocene. Second, all reconstructions are characterized by a steep section of the age-paleodepth curve from approximately 15-20 Ma over an elevation range of at minimum 1 km, indicating an episode of rapid cooling during the Early to Mid-Miocene. Third, in all reconstructions the two easternmost samples of Mid-Tertiary age lie off the general trend, helping to delineate the location of the Blue River fault and enabling an estimate of fault offset magnitude. Finally, the presence of Mid-Tertiary dates in the profile, and the absence of Early Tertiary and older results, is strikingly different from the pattern of AFT results in adjacent ranges.

7.2 Late Cenozoic unroofing history

In a pattern similar to other rift flank uplifts, cooling ages in the Gore Range young towards the major basin-bounding fault. The youngest date of 6.9 ± 2.8 Ma is found at the southeastern boundary of the range. Using a range of geothermal gradients from 30-40 °C/km consistent with the modern geothermal gradient of 35 °C/km (Nathenson and Guffanti, 1988), applying an annual surface temperature of 10 °C, and assuming monotonic cooling with a closure temperature of 70 °C, this youngest date implies 1.5-2 km unroofing on the eastern edge of the Gore Range since the Late Miocene. Assuming that the modern geothermal gradient has remained constant since the Miocene, the average cooling rate since the Late Miocene is about 9 °C/Ma.

The ages invariant within error and steep slope of the age-elevation plot between 15 and 20 Ma strongly suggests a rapid cooling episode in the Gore Range during the Early to Mid-Miocene. In the absence of another cause for rapid cooling, this pattern is indicative of samples that were exhumed rapidly through the helium closure temperature at approximately the same time (Spotila, 2005). In general, samples that experienced monotonic cooling collected over a range of elevations are expected to yield an age distribution that plots as either a shallow or steep line on an age-elevation or age-paleodepth graph (Harrison and Zeitler, 2005; Figure 5). A line of flat or shallow slope is relatively elevation-invariant and indicates that retention of ^{4}He across the sampled elevation range changed slowly or not at all; this pattern will develop when samples have spent a prolonged period in the partial retention zone. Slow, steady cooling will create a moderate slope and a steep line that is close to age-invariant indicates the scenario where the rate of retention of ^{4}He changes rapidly with elevation (Harrison and Zeitler, 2005; Spotila, 2005). This latter pattern is observed for the 15-20 Ma Gore Range samples over a depth range of about 1 km.

Assuming the modern geothermal gradient of 35° C/km, samples on the eastern edge of the Gore Range cooled at a rate of at least 9 °C/Ma during the Early to Mid-Miocene. On the age-paleodepth plots with structural tilts of at least 15° there is a break in slope at ~15 Ma and a shallowing of the age-elevation slope to ~7 Ma. This suggests a possible deceleration of cooling between 15 and 7 Ma. If a period of slower cooling did occur, then at some time between 7 Ma and the present rapid cooling must have resumed in order to account for the more recent 9 °C/Ma cooling rate derived at the beginning of this section.

The Blue River fault has been mapped as a zone of faulting up to 1 km wide (West, 1978) along the eastern edge of the range. The two eastern samples with Mid-Tertiary dates are all located within or to the east of that zone. These results more clearly define the location of the major strand of the Blue River fault. We sampled basement rocks on both sides of the fault at two locations. Samples within 100 m of the same elevation on different sides of the fault yielded dates offset by 23 and 24 Ma. The position of the two easternmost samples and their location off the general age-elevation trend in all the profiles confirm that the two samples in this group have experienced a cooling history since the Mid-Tertiary that is different from the samples in the main Gore Range fault block. As part of a separate fault block or blocks, the degree of structural tilt that the two samples experienced must be different than the other two sample groups. Given the small number of samples in this group, the data does not tightly constrain the cooling history of these fault blocks. However, sample L09-BL4 is located in an area of the range near samples GRWL10 and GRWL12, both of which are of a similar age. The offset between these samples is 1.4 km at a minimum structural tilt of 10°. At a structural tilt of 20° the offset on the Blue River fault is at least 2.7 km.

The AFT data for this set of samples was published by C. Naeser and others in 2002 (Appendix 1). The dataset suggested cooling in the Gore Range at ~30 Ma due to prior elevated heat flow, followed by continued rapid cooling through the Miocene and into the Pliocene. The anomalously young cooling ages in the Gore Range and the pattern of younging towards the basin-bounding fault confirmed that the range is a flank uplift of the Rio Grande Rift. The data presented in this paper leads to the same first order conclusions, but expands this history to lower temperatures. A discrepancy between the AFT and (U-Th)/He dates prevents detailed thermal modeling using both thermochronometers. Samples in the eastern Gore Range have identical AFT and (U-Th)/He dates within error. Four samples in the western Gore Range have AFT dates that are 8-17 Ma younger than the (U-Th)/He dates. Samples with this discrepancy had some of the highest quality apatite grains in the study and there is no statistically significant eU correlation in any sample. The discrepancy is currently unexplained.

7.3 Mid-Tertiary thermal history: signature of unroofing or elevated geotherms?

Mid-Tertiary (U-Th)/He dates and previously reported Mid-Tertiary AFT dates (Naeser et al., 2002) from the western Gore Range contrast with the Late Cretaceous and Early Tertiary AFT dates in the nearby Front Range, Park Range, and White River uplift. Instead, a similar Mid-Tertiary signature has been identified in rift flank uplifts bounding the major basins of the Rio Grande Rift in southern Colorado and New Mexico (e.g. Kelley et al., 1992; House et al., 2003). Whether the Mid-Tertiary dates are primarily attributable to cooling due to unroofing or in part reflect the elevation of Mid-Tertiary geotherms, their presence is important for understanding rift evolution.

Mid-Tertiary cooling due to unroofing at this time is compatible with sedimentary evidence in the Blue River Valley and surrounding areas suggesting some unroofing of the Gore Range prior to 27 Ma. A section of Mid-Tertiary sedimentary rocks in the Blue River Valley contains a basal boulder conglomerate overlain by a 27 Ma tuff; clasts in the conglomerate are made of the granite and migmatitic biotite gneiss found in the surrounding ranges. Above the boulder conglomerate the section is composed of tuff, shale, siltstone, and limestone capped by 24 Ma flows of trachyandesite (Naeser et al., 2002). The existence of this conglomerate requires that some degree of relief had been generated between the Blue River Valley and a neighboring range prior to 27 Ma. This sedimentary section is similar to synrift units elsewhere in the rift system. Possibly similar outcrops near Climax, Colorado, have led to speculation that Oligocene fill of this type may once have been continuous from the Upper Arkansas Valley through the Blue River Valley and into Middle Park (Tweto, 1979). Thus, in the northern Rio Grande Rift, the absence of synrift sedimentary deposits like those in the rift basins of southern

Colorado and New Mexico may be a consequence of erosion rather than lack of deposition. The ~24 Ma basal conglomerates in the Browns Park Formation west of the Park Range have also been linked to the generation of relief during the Oligocene between that valley and the neighboring range (Izett, 1975; Larson et al., 1975). Unroofing linked to the development of this relief should have left a cooling signature in affected rocks. A steep slope on the age-paleodepth reconstructions between samples GRWL10 and GRWL12 in the central Gore Range at ~30 Ma is consistent with rapid cooling during Oligocene unroofing. Similar dates from the two easternmost samples could indicate that they experienced this event as well.

Whether the Mid-Tertiary dates in part reflect elevated geotherms in Mid-Tertiary time remains an intriguing, but still open, question. Naeser and others (2002) used the existence of Mid-Tertiary AFT dates in the northern Gore Range to suggest that cooling at 30 Ma was preceded by an episode of heating due to elevated geothermal gradients. They note that a sample with an AFT date of ~20 Ma came from a location in the northern Gore Range just 200 m below the Mesozoic sedimentary section. If the maximum possible latest Paleozoic to Mesozoic sedimentary section – a thickness of ~3.3 km (Kellogg, unpub.) – was preserved above this sample at 20 Ma and the sample was 200 m below the base of that section, then assuming a surface temperature of 10 °C and a total AFT resetting temperature of 120 °C, at 20 Ma the geothermal gradient at this location was 31 °C/km. However, Naeser and others (2002) point out that much of the sedimentary section was probably eroded off the range during the Laramide orogeny. They further note that this would leave the sample with a Laramide or older age unless elevated geothermal gradients high enough to reset it affected the area in the Mid-

Tertiary. While this particular sample underlies only the Jurassic Morrison Formation, units as young as the Cretaceous Dakota Group are preserved nearby on the range. In contrast, the entire sedimentary section had been eroded from much of the Front Range by the end of the Cretaceous; Proterozoic clasts shed from the range appear in the Arapahoe Formation of the Denver Basin at this time (Naeser et al., 1980; Raynolds et al., 2007). Since at least some of the section was preserved in the northern Gores, if we assume that all of the formations above the Dakota Group – the easily erodible Benton Group, Niobrara Formation, and Pierre Shale – were removed during the Laramide then at the end of that time this sample was sitting at a depth of no more than 500 m. Reheating it to the point of total resetting at this depth because of elevated geothermal gradients would require unreasonably high heat flow. There is also no known intrusive or volcanic unit near enough to the sample to have this effect. Assuming a surface temperature of 10 °C, even the very high geothermal gradient of 45 °C/km would have required at least 1.2 km of Pierre Shale to have been preserved on top of the sedimentary section at this location at the end of the Laramide orogeny. In order to better understand the contribution of elevated geotherms to the Mid-Tertiary cooling history of the region, samples for future (U-Th)/He analysis have been collected both in and just below the sedimentary section in the northern Gores.

A linkage between widespread Mid-Tertiary volcanism and an increase in crustal geotherms has been proposed in southern Colorado and New Mexico (e.g., Roy et al., 2004), but Mid-Tertiary magmatism was more limited in central Colorado. Figure 9 summarizes patterns of volcanic and intrusive activity in the Rio Grande Rift region from the Eocene to the present. In and near the Gore Range there are the ~32 Ma intrusive

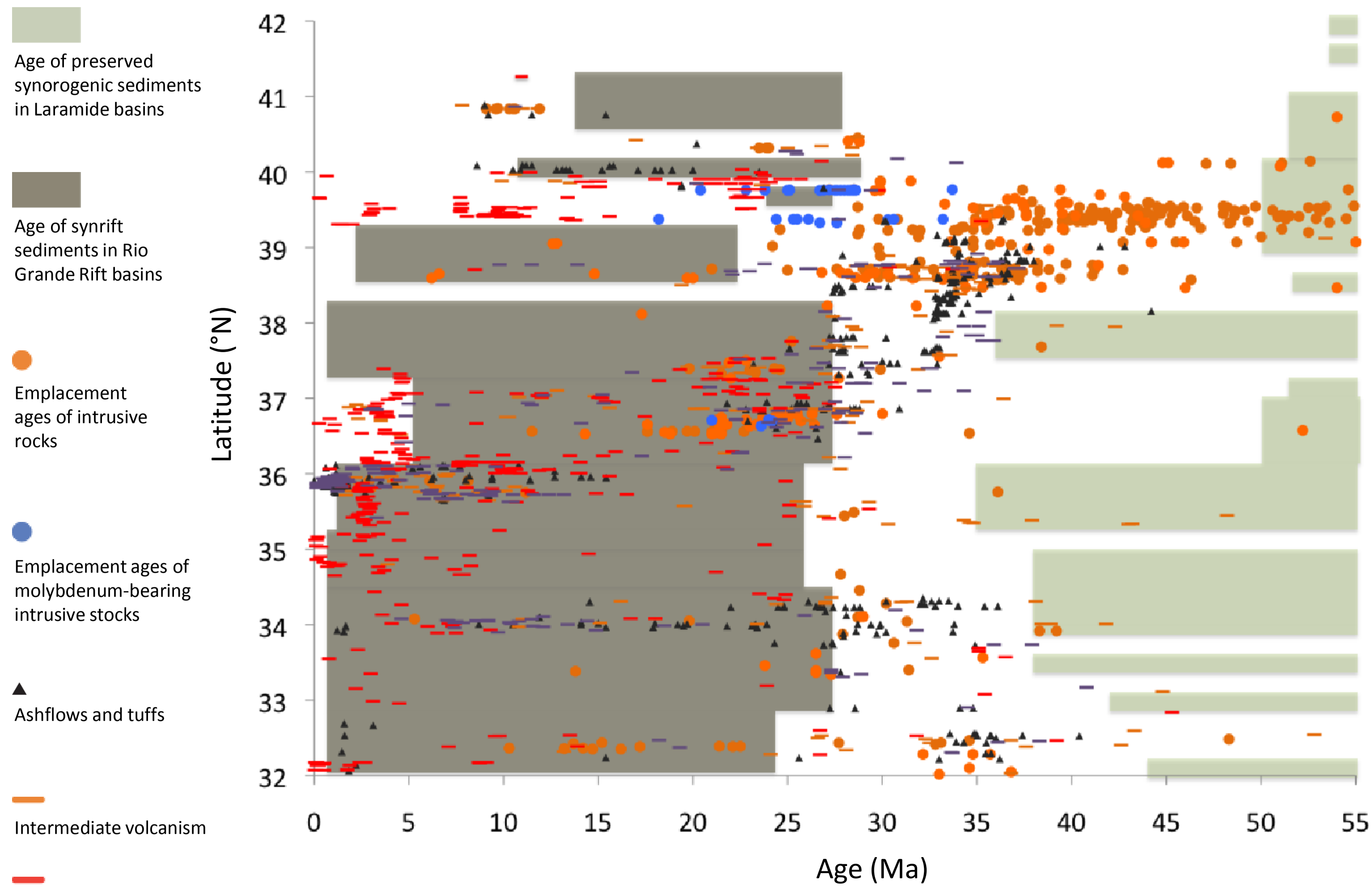

Figure 9: Compilation of post- 55 Ma stratigraphic and geochronological constraints on the depositional history of Laramide and Rio Grande rift basins and the timing and patterns of intrusive and volcanic activity. Area spans a latitude range of 104.8 – 107.5 W. Ages from Cather and Chapin, 1990; Chapin and Cather, 1994; Dickinson et al, 1988; Izett, 1975; Klein et al, 2009; Lawton, 2008; Wilks and Chapin, 1997.

stock and ~24 Ma volcanic flows in the Blue River Valley, in addition to some undated dikes that are thought to be Oligocene or Miocene in the southern Gore Range (Naeser et al., 2002). Undated basalts overlie Proterozoic and younger units in the northern Gore Range. These volcanics have been linked to the 24-20 Ma set of basalt flows to the west of the Gore Range in the Yarmony Mountain-State Bridge-Piney Ridge area (Larson et al., 1975; Kunk et al., 2002). The Colorado Mineral Belt extends from the Tenmile Range into the Front Range across the Upper Blue River Valley south of the Gore Range. During the Mid-Tertiary numerous intrusions such as the 38 Ma Montezuma stock and 44 Ma Swan Mountain stock (Marvin et al, 1989) were emplaced in the Mineral Belt near the study area. Naeser and others (2002) note that AFT dates taken from samples in the Front Range not far from these intrusives do not appear to have been reset when they were emplaced. The 24-33 Ma Climax and Red Mountain molybdenum-bearing intrusives (Bookstrom et al., 1988) in the Mosquito and Front Ranges are also close to the study area, along with smaller 35-44 Ma intrusives in Paleozoic rocks in the northern Sawatch range (Mach and Thompson, 1998). Further to the south, a period of intense magmatism began with the eruption of the Wall Mountain Tuff from the Mt. Princeton area in the southern Sawatch Range at 36.7 Ma (McIntosh and Chapin, 2004). Volcanic eruptions and the development of the Mt. Princeton batholith continued until ~30 Ma (Shannon, 1988; McIntosh and Chapin, 2004).

7.4 Implications for the evolution of the northern Rio Grande Rift

The cooling history of the Gore Range is notably similar to cooling histories inferred for rift flank uplifts further to the south in the Rio Grande Rift. Volcanic units interbedded with synrift sedimentary deposits date the initiation of rifting to approximately 26-29 Ma in the San Luis, Española, Albuquerque and Popotosa Basins (Chapin and Cather, 1994; Miggins et al., 2002). Three observations point toward a similar timing for the onset of rifting by 27 Ma in the Blue River Valley. First, a 26.9 ± 0.06 Ma welded tuff overlying a basal conglomerate similar to synrift units elsewhere in the rift system (Naeser et al., 2002) imposes a minimum age for the initiation of rifting in the Blue River Valley. Second, Climax-type molybdenum deposits, found only in continental rift settings (Ludington and Plumlee, 2009), were emplaced beginning at 33 Ma near the Blue River Valley. Finally, our (U-Th)/He data are suggestive of an early Oligocene cooling event, consistent with the onset of rifting at this time.

After initiation of rifting in the Oligocene, the stratigraphic record indicates that rates of extension increased throughout the rift during the Mid- to Late Miocene before slowing again to the present (e.g., Chapin and Cather, 1994). In the Sandia Mountains flanking the Albuquerque basin cooling rates were derived from a combination of apatite fission-track and (U-Th)/He thermochronology. These dates record fast cooling from 22-17 Ma followed by slower cooling to 16 Ma, a short increase in cooling rate at 14 Ma, and then slower cooling to the present (House et al., 2003). AFT dates in the Sangre de Cristo Range bordering the San Luis Basin indicate rapid cooling at ~15 Ma (Kelley et al., 1992). $^{40}Ar/^{39}Ar$ geochronology from offset volcanic rocks in the San Luis Basin and southern Sangre de Cristo Range reveal this same Mid-Miocene unroofing event (Miggins et al., 2002).

The Early to Mid-Miocene rapid cooling at the eastern edge of the Gore Range overlaps with both the Early Miocene rapid cooling in the Sandias and the Mid-Miocene cooling and unroofing in the Sangre de Cristo Range. The inflection point in the paleodepth profiles may correspond to the slower extension rates seen throughout the rift in Late Miocene to Pliocene time (Chapin and Cather, 1994; Lozinsky, 1994; Cather et al., 1994). Consistent cooling ages from as far south as Socorro, New Mexico, to the Blue River Valley suggest that the rift north of the San Luis Basin has experienced a history consistent with rift basins to the south. There is no evidence for significant northward propagation of the Rio Grande Rift. Instead, cooling ages in the Gore Range suggest the broadly synchronous onset and evolution of a >700 km segment of this major intracontinental rift.

8. Conclusions

This study constrains the Mid- to Late Cenozoic cooling and unroofing history of a northern Rio Grande Rift flank uplift. Unlike neighboring ranges, low temperature thermochronology data for the Gore Range in central Colorado preserves no history of Early Tertiary or older cooling. Instead, more recent exhumation has brought the signatures of much younger cooling events to the surface.

A two-stage unroofing history of the Gore Range can provide a plausible explanation of both the age-elevation relationships in the southern Gores and the profound geomorphic contrast between that area and the northern Gores. At ~30 Ma the entire range may have experienced cooling due to unroofing, with a possible contribution from elevated heat flow. By 27 Ma some relief existed between the Gore Range and the Blue River Valley. A small quantity of synrift sediment from that time is preserved in the Blue River Valley, and it is possible that this was part of more extensive fill that was later removed by the Colorado River system. During the Early and Mid-Miocene rapid cooling and unroofing was likely restricted to the southern Gores. The cross fault dividing the northern and southern Gores accommodated down-to-the-north extension as movement on the Blue River normal fault caused unroofing and elevation gain in the southern Gores, also stripping them of any remaining sedimentary or volcanic cover. Rapid cooling and associated unroofing continued in the range until at least the Late Miocene. Apatite (U-Th)/He dates from the Gore Range demonstrate that significant rock exhumation occurred in the central Colorado Rocky Mountains during the Late Cenozoic due to the effects of Rio Grande Rift.

9. Future Work

Work is currently in progress to obtain (U-Th)/He dates for 1) basement rocks and sedimentary cover in the northern Gores and 2) basement rocks from Gore Canyon. Data from the northern Gores will test the two-stage cooling history inferred from our southern Gore dataset and better tie the cooling history of the Gore Range to the rest of the Rocky Mountains. The Colorado River incised the 500 m deep Gore Canyon and data from that location may shed light on how the integration of the river is linked with the evolution of the Blue River Valley.

References

Bookstrom, A.A., Carten, R.B., Shannon, J.R., Smith, R.P., 1988, Origins of bimodal leucogranite-lamprophyre suites, Climax and Red Mountain porphyry molybdenum systems, Colorado: Petrologic and strontium isotopic evidence, in, Drexler, J.W. and Larson, E.E., eds., Cenozoic volcanism in the southern Rocky Mountains revisited, Colorado School of Mines Quarterly, v. 83, no. 2, pt. 3, p. 1-22.

Brister, B.S. and Gries, R.R., 1994, Tertiary stratigraphy and tectonic development of the Alamosa Basin (Northern San Luis Basin), Rio Grande Rift, south-central Colorado, in, Keller, G.R. and Cather, S.M., eds, Basins of the Rio Grande Rift: Structure, Stratigraphy and Tectonic Setting, Geological Society of America Special Paper 291, p. 39-58.

Bryant, B. and Naeser, C.W., 1980, The significance of fission-track ages of apatite in relation to the tectonic history of the Front and Sawatch ranges, Colorado, Geological Society of America Bulletin, v. 91, no. 3, p. 156-164.

Bryant, B., Naeser, C.W, Stegen, R.J., 1990, Reconnaissance fission-track geochronology of the Aspen mining district, central Colorado, in, Beaty, D.W, Landis, G.P., Thompson, T.B., eds., Carbonate-hosted sulfide deposits of the central Colorado mineral belt, Economic Geology Monographs, v. 7, p. 301-307.

Cather, S.M., Chapin, C.E., 1990, Paleogeographic and paleotectonic setting of Laramide sedimentary basins in the central Rocky Mountain region: alternative interpretation, Geological Society of America Bulletin, v.102, no. 2, p. 256-258.

Cather, S.M., Chamberlin, R.M., Chapin, C.E., McIntosh, W.C., 1994, Stratigraphic consequences of episodic extension in the Lemitar Mountains, central Rio Grande Rift, in, Keller, G.R. and Cather, S.M., eds, Basins of the Rio Grande Rift: Structure, Stratigraphy and Tectonic Setting: Geological Society of America Special Paper 291, p. 157-170.

Chamberlain, K.R., 1998, Medicine Bow orogeny: timing of deformation and model of crustal structure produced during continent-arc collision, ca. 1.78 Ga, southeastern Wyoming, Rocky Mountain Geology, v. 33, no. 2, p. 259 – 277.

Chapin, C.E. and Cather, S.M., 1994, Tectonic settings of the axial basins of the northern and central Rio Grande rift, in, Keller, G.R. and Cather, S.M., eds, Basins of the Rio Grande Rift: Structure, Stratigraphy and Tectonic Setting: Geological Society of America Special Paper 291, p. 5 – 26.

Church, S.E. and Bickford, M.E., 1971, Spontaneous fission-track studies of accessory apatite from granitic rocks of the Sawatch range, Colorado, Geological Society of America Bulletin, v. 82, no. 6, p. 1727-1733.

Crowley, P.D., Reiners, P.W., Reuter, J.M., Kaye, G.D., 2002, Laramide exhumation of the Bighorn Mountains, Wyoming; an apatite (U-Th)/He thermochronology study, *Geology,* v. 30, no. 1, p. 27-30.

Dickinson, W.R., Klute, M.A., Hayes, M.J., Janecke, S.U., Lundin, E.R., McKittrick, M.A., Olivares, M.D., 1988, Paleogeographic and paleotectonic setting of Laramide sedimentary basins in the central Rocky Mountain region, Geological Society of America Bulletin, v. 100, no. 7, p. 1023 – 1039.

Donelick, R.A., O'Sullivan, P.B., Ketcham, R.A., 2005, Apatite fission-track analysis, in, Reiners, P.W. and Ehlers, T.A., eds., Low-temperature thermochronology; techniques, interpretations, and applications, Reviews in Mineralogy and Geochemistry, v. 58, no. 1, p. 49 – 94.

Dunai, T.J., 2005, Forward modeling and interpretation of (U-Th)/He ages, in, Reiners, P.W. and Ehlers, T.A., eds., Low-temperature thermochronology; techniques, interpretations, and applications, Reviews in Mineralogy and Geochemistry, v. 58, no. 1, p. 259-274.

Eaton, G.P., 1986, A tectonic redefinition of the southern Rocky Mountains, Tectonophysics, v. 132, no. 1-3, p. 163 – 193.

Ehlers, T.A., 2005, Crustal thermal processes and the interpretation of thermochronometer data, in, Reiners, P.W. and Ehlers, T.A., eds., Low-temperature thermochronology; techniques, interpretations, and applications, Reviews in Mineralogy and Geochemistry, v. 58, no. 1, p. 315-350.

Epis, R.C., and Chapin, C.E., 1975, Geomorphic and tectonic implications of the post-Laramide, late Eocene erosion surface in the southern Rocky Mountains, in, Curtis, B.F., ed., Cenozoic history of the southern Rocky Mountains, Geological Society of America Memoir 144, p. 45 – 74.

Erslev, E.A., Kellogg, K.S., Bryant, B., Ehrlich, T.K., Holdaway, S.M., Naeser, C.W., 1999, Laramide to Holocene structural development of the northern Colorado Front Range, in, Lageson, D.R. et al., eds., Colorado and adjacent areas, Geological Society of American Field Guide 1, p. 21 – 40.

Farley, K.A., Wolf, R.A., Silver, L.T., 1996, The effects of long alpha-stopping distances on (U-Th)/He ages, Geochimica et Cosmochimica Acta, v. 60, p. 4223-4229.

Farley, K., 2000, Helium diffusion from apatite; general behavior as illustrated by Durango fluorapatite, Journal of Geophysical Research, v. 105, p. 2903 – 2914.

Fisher, L.R., and Fisher, T.R., Continental accretion, Colorado style: Proterozoic island arcs and backarcs of the central Front Range, in, Nelson, E.P. and Erslev, E.A., eds., Field trips in the southern Rocky Mountains, USA, Geological Society of America Field Guide 5, p. 109 – 129.

Flowers, R.M., Ketcham, R.A., Shuster, D.L., Farley, K.A., 2009, Apatite (U–Th)/He thermochronometry using a radiation damage accumulation and annealing model, Geochimica et Cosmochimica Acta, v. 73, p. 2347-2365.

Green, G.N., 1992, The digital geologic map of Colorado in ARC/INFO format, U.S. Geological Survey Open-File Report 92-0507.

Green, G.N. and Jones, G.E., 1997, The digital geologic map of New Mexico in ARC/INFO format, U.S. Geological Survey Open-File Report 97-0052.

Gregory, K.M. and Chase, C.G., 1992, Tectonic significance of paleobotanically estimated climate and altitude of the late Eocene erosion surface, Colorado, Geology, v. 20, no. 7, p. 581-585.

Harrison, T.M. and Zeitler, P.K., 2005, Fundamentals of noble gas thermochronometry, in, Reiners, P.W. and Ehlers, T.A., eds., Low-temperature thermochronology; techniques, interpretations, and applications, Reviews in Mineralogy and Geochemistry, v. 58, no. 1, p. 49-94.

House, M.A., Farley, K.A., Stockli, D., 2000, Helium chronometry of apatite and titanite using Nd-YAG laser heating, Earth and Planetary Science Letters, v. 183, no. 3-4, p. 365-368.

House, M.A., Kelley, S.A., Roy, M., 2003, Refining the footwall cooling history of a rift flank uplift, Rio Grande rift, New Mexico, *Tectonics*, v. *22,* no. 5, p. 1060-1078.

Hoy, R.G., and Ridgway, K.D., 2002, Syndepositional thrust-related deformation and sedimentation in an Ancestral Rocky Mountains basin, Central Colorado Trough, Colorado, USA, Geological Society of America Bulletin, v. 114, no. 7, p. 804 – 828.

Ingersoll, R.V., 2001, Structural and stratigraphic evolution of the Rio Grande Rift, northern New Mexico and southern Colorado, International Geology Review, v. 43, no. 10, p. 867-891.

Izett, G.A., 1975, Late Cenozoic sedimentation and deformation in northern Colorado and adjoining areas, in, Curtis, B.F., ed., Cenozoic history of the southern Rocky Mountains, Geological Society of America Memoir 144, p. 179 – 209.

Karlstrom, K.E., Kirby, E., Kelley, S.A., Aslan, A., Sandoval, M.M., Crow, R.S., 2007, Neotectonic influences on the longitudinal profile of the Colorado River system in Grand Canyon and the Rocky Mountains, Abstracts with Programs - Geological Society of America, v. 39, no. 6, p. 194.

Keller, G.R. and Baldridge, W.S., 1999, The Rio Grande Rift: a geological and geophysical overview, Rocky Mountain Geology, v. 34, n. 1, p. 121-130.

Kelley, S.A. and Duncan, I.J., 1986, Late Cretaceous to middle Tertiary tectonic history of the northern Rio Grande Rift, New Mexico, Journal of Geophysical Research, v. 91, no. B6, p. 6246-6262.

Kelley, S.A., Chapin, C.E., Corrigan, J., 1992, Late Mesozoic to Cenozoic cooling histories of the flanks of the northern and central Rio Grande Rift, Colorado and New Mexico, Bulletin - New Mexico Bureau of Geology & Mineral Resources, Report 145.

Kelley, S.A, and Chapin, C.E., 1995, Apatite fission-track thermochronology mapping in the Southern Rocky Mountains-Rio Grande Rift province, AAPG Bulletin, v. 79, no. 6, p. 920.

Kelley, S.A. and Chapin, C.E., 1997, Cooling histories of mountain ranges in the southern Rio Grande Rift based on apatite fission-track analysis; a reconnaissance survey, New Mexico Geology, v. 19, no. 1, p.1-14.

Kelley, S.A., 2002, Unroofing of the southern Front Range, Colorado; a view from the Denver Basin, Rocky Mountain Geology, v. 37, no. 2, p. 189 – 200.

Kelley, S.A. and Chapin, C.E., 2004, Denudation history and internal structure of the Front Range and Wet Mountains, Colorado, based on apatite-fission-track thermochronology, New Mexico Bureau of Geology and Mineral Resources Bulletin 160, p. 41-77.

Kelley, S.A., 2005, Low-temperature cooling histories of the Cheyenne Belt and Laramie Peak Shear Zone, Wyoming, and the Soda Creek-Fish Creek Shear Zone, Colorado, in, Karlstrom, K.E. and Keller, R.G., eds., The Rocky Mountain Region – An Evolving Lithosphere: Tectonics, Geochemistry, and Geophysics, Geophysical Monograph 154, p. 55-70.

Kellogg, K.S., 1999, Neogene basins of the Northern Rio Grande rift: partitioning and asymmetry inherited from Laramide and older uplifts, *Tectonophysics,* v. *305*, p. 141-152.

Kellogg, K.S., Bartos, P.J., Williams, C.L., 2002, Geologic map of the Frisco Quadrangle, Summit County, Colorado, U.S. Geological Survey Miscellaneous Field Studies Map MF-2340.

Kellogg, K.S., Bryant, B., Redsteer, M.H., 2003, Geologic map of the Vail East Quadrangle, Eagle County, Colorado, U.S. Geological Survey Miscellaneous Field Studies Map MF-2375.

Kellogg, K.S., Bryant, B., Reed, J.C., 2004, The Colorado Front Range – anatomy of a Laramide uplift, in, Nelson, E.P. and Erslev, E.A., eds., Field trips in the southern Rocky Mountains, USA, Geological Society of America Field Guide 5, p. 89-108.

Klein, T.L., Evans, K.V., DeWitt, E.H., 2009, Geochronology database for central Colorado, U.S. Geological Survey Data Series 489.

Kluth, C.F. and Schaftenaar, C.H., 1994, Depth and geometry of the northern Rio Grande Rift in the San Luis Basin, south-central Colorado, in, Keller, G.R. and Cather, S.M., eds, Basins of the Rio Grande Rift: Structure, Stratigraphy and Tectonic Setting: Geological Society of America Special Paper 291,p. 27 – 38.

Kunk, M.J., Budahn, J.R., Unruh, J.M., Stanley, J.O., Kirkham, R.M., Bryant, B., Scott, R.B., Lidke, D.J., Streufert, R.K., 2002, 40Ar/39Ar ages of late Cenozoic volcanic rocks within and around the Carbondale and Eagle collapse centers, Colorado: Constraints on the timing of evaporite-related collapse and incision of the Colorado River, *In*: Kirkham, R.M., Scott, R.B., Judkins, T.W., eds., Late Cenozoic evaporite tectonism and volcanism in west-central Colorado, *Geological Society of America Special Paper 366*, p. 213-234.

Larson, E.E., Ozima, M., Bradley, W.C., 1975, Late Cenozoic basic volcanism in northwestern Colorado and its implications concerning tectonism and the origin of the Colorado River system, in, Curtis, B.F., ed., Cenozoic history of the southern Rocky Mountains, Geological Society of America Memoir 144, p. 155-178.

Lawton, T.F., 2008, Laramide sedimentary basins, in Miall, A.D., ed., The sedimentary basins of the United States and Canada: Sedimentary basins of the world, Elsevier, Amsterdam, p. 429-450.

Leonard, E.M., 2002, Geomorphic and tectonic forcing of late Cenozoic warping of the Colorado piedmont, Geology, v. 30, no. 7, p. 595-598.

Lewis, C.J. and Baldridge, W.S., 1994, Crustal extension in the Rio Grande Rift, New Mexico: half-grabens, accommodation zones, and shoulder uplifts in the Ladron Peak-Sierra Lucero area, in, Keller, G.R. and Cather, S.M., eds, Basins of the Rio Grande Rift: Structure, Stratigraphy and Tectonic Setting, Geological Society of America Special Paper 291, p. 135-156.

Lindsey, D.A., Andriessen, P.A.M., Wardlaw, B.R., 1986, Heating, cooling, and uplift during Tertiary time, northern Sangre de Cristo Range, Colorado, Geological Society of America Bulletin, v. 97, p. 1133-1143.

Lipman, P.W., and Mehnert, H.H., 1975, Late Cenozoic volcanism and development of the Rio Grande depression in the southern Rocky Mountains, in, Curtis, B.F., ed., Cenozoic history of the southern Rocky Mountains, Geological Society of America Memoir v. 144, p. 119 – 154.

Lipman, P.W., Mehnert, H.H., Naeser, C.W., 1986, Evolution of the Latir volcanic field, northern New Mexico, and its relation to the Rio Grande Rift, as indicated by potassium-argon and fission track dating, Journal of Geophysical Research, v. 91, no. B6, p. 6329-6345.

Lozinsky, R.P., 1994, Cenozoic stratigraphy, sandstone petrology, and depositional history of the Albuquerque Basin, central New Mexico, in, Keller, G.R. and Cather, S.M., eds, Basins of the Rio Grande Rift: Structure, Stratigraphy and Tectonic Setting: Geological Society of America Special Paper 291, p. 73 -82.

Ludington, S.L. and Plumlee, G.S., 2009, Climax-type porphyry molybdenum deposits: USGS Open-File Report 2009-1215.

Mach, C.J. and Thompson, T.B., 1998, Geology and geochemistry of the Kokomo mining district, Colorado, Economic Geology, v. 93, p. 617-638.

Manning, A.H. and Caine, J.S., 2007, Groundwater noble gas, age, and temperature signatures in an alpine watershed: valuable tools in conceptual model development, Water Resources Research, v. 43, p. 1-16.

Marvin, R.F. and Dobson, S.W., 1979, Radiometric ages; compilation B, U. S. Geological Survey Isochron/West, no. 26, p.3-30.

Marvin, R.F., Mehnert, H.H, Naeser, C.W., Zartman, R.E., 1989, U.S. Geological Survey radiometric ages: Compilation C, Part five: Colorado, Montana, Utah and Wyoming, Isochron/West, no. 53, p. 14-22.

McIntosh, W.C. and Chapin, C.E., 2004, Geochronology of the central Colorado volcanic field, New Mexico Bureau of Geology and Mineral Resources Bulletin 160, p. 205-238.

McMillan, M.E., Angevine, C.L., Heller, P.L., 2002, Postdepositional tilt of the Miocene-Pliocene Ogallala Group on the western Great Plains; evidence of late Cenozoic uplift of the Rocky Mountains, Geology, v. 30, no. 1, p.63-66, Jan 2002.

McMillan, M.E., Heller, P.L., Wing, S.L., 2006, History and causes of post-Laramide relief in the Rocky Mountain orogenic plateau, *GSA Bulletin*; March 2006; v. 118; no. 3-4; p. 393-405.

Miggins, D.P., Thompson, R.A., Pillmore, C.L., Snee, L.W., Stern, C.R., 2002, Extension and uplift of the northern Rio Grande Rift: Evidence from $^{40}Ar/^{39}Ar$ geochronology from the Sangre de Cristo Mountains, south-central Colorado and northern New Mexico, in, Menzies, M.A., Klemperer, S.L., Ebinger, C.J., Baker, J., eds., Volcanic Rifted Margins, Geological Society of America Special Paper 362, p. 47-64.

Naeser, C.W., 1971, Geochronology of the Navajo-Hopi diatremes, Four Corners area, Journal of Geophysical Research, v. 76, no. 20, p. 4978-4985.

Naeser, C.W., Cunningham, C.G., Beaty, D.W., 1990, Origin of the ore deposits and Giman, Colorado; Part III, Fission-track and fluid inclusion studies, Economic Geology Monographs, v. 7, p. 219-228.

Naeser, C.W., Bryant, B. Kunk, M.J., Kellogg, K., Donelick, R.A., Perry, W.J., 2002, Tertiary cooling and tectonic history of the White River uplift, Gore Range, and western Front Range, central Colorado: Evidence from fission-track and 39Ar/40Ar ages, *In*: Kirkham, R.M., Scott, R.B., Judkins, T.W., eds., Late Cenozoic evaporite tectonism and volcanism in west-central Colorado, Geological Society of America Special Paper 366, p. 31-53.

Nathenson, M. and Guffanti, M., 1988, Geothermal gradients in the conterminous United States, Journal of Geophysical Research, v. 93, p. 6437-6450.

Obradovich, J. D., 1993, A Cretaceous time scale, in, Caldwell, W. G. E., and Kauffman, E. G., eds., Evolution of the Western Interior Basin, Geological Association of Canada Special Paper 39, p. 379–396.

Olson, J.C., Marvin, R.F., Parker, R.L., Mehnert, H.H., 1977, Age and tectonic setting of lower Paleozoic alkalic and mafic rocks, carbonatites, and thorium veins in South-central Colorado, Journal of Research of the U. S. Geological Survey, v .5, no. 6, p. 673-687.

Raynolds, R.G., Johnson, K.R., Ellis, B., Dechesne, M., Miller, I.M., 2007, Earth history along Colorado's Front Range: Salvaging geologic data in the suburbs and sharing it with citizens, GSA Today, v. 17, no. 12, p. 4 – 10.

Roy, M., Kelley, S., Pazzaglia, F., Cather, S., House, M., 2004, Middle Tertiary buoyancy modification and its relationship to rock exhumation, cooling, and subsequent extension at the eastern margin of the Colorado Plateau, Geology, v. 32, no. 10, p. 925-928.

Reiners, P.W., 2009, Nonmonotonic thermal histories and constrasting kinetics of multiple thermochronometers, Geochimica et Cosmochimica Acta, v. 73, p. 3612-3629.

Shannon, J.R., 1988, Geology of the Mount Aetna cauldron complex, Sawatch Range, Colorado, Ph.D. Thesis, Colorado School of Mines, Golden, CO.

Shuster, D.L. and Farley, K.A., 2005, 4He/3He thermochronometry: theory, practice and potential complications, in, Reiners, P.W. and Ehlers, T.A., eds., Low-temperature thermochronology; techniques, interpretations, and applications, Reviews in Mineralogy and Geochemistry, v. 58, no. 1, p. 181-203.

Spotila, J.A., 2005, Applications of low-temperature thermochronometry to quantification of recent exhumation in mountain belts, in, Reiners, P.W. and Ehlers, T.A., eds., Low-temperature thermochronology; techniques, interpretations, and applications, Reviews in Mineralogy and Geochemistry, v. 58, no. 1, p. 449-466.

Tweto, O., Bryant, B., Williams, F.E., 1970, Mineral resources of the Gore Range – Eagle's Nest primitive area and vicinity, Summit and Eagle Counties, Colorado, U. S. Geological Survey Bulletin, Report: B, 1319-C, p. 1-127.

Tweto, O., 1979, The Rio Grande Rift system in Colorado, in, Riecker, R.E., ed., Rio Grande Rift: Tectonics and Magmatism, American Geophysical Union, Washington, D.C., p. 33-56.

Tweto, O., 1987, Rock units of the Precambrian basement in Colorado, U. S. Geological Survey Professional Paper, Report: P, 1321-A, p. 1-54.

Wallace, C.A., Keller, J.W., McCalpin, J.P., Bartos, P.J., Route, E.E., Jones, N.N., Gutierrez, F., Williams, C.L., Morgan, M.L., 2003, Geologic map of the Breckenridge quadrangle, Summit and Park Counties, Colorado, Colorado Geological Survey Open-File Report 02-7.

West, M.W., 1978, Quaternary geology and reported surface faulting along along east flank of Gore Range, Summit County, Colorado, Quarterly of the Colorado School of Mines, v. 73, no. 2.

West, M., Ni, J., Baldridge, W.S., Wilson, D., Aster, R., Gao, W., 2004, Crust and upper mantle shear wave structure of the southwest United States: Implications for rifting and support for high elevation, Journal of Geophysical Research, v. 109, p. 16.

Wilks, M. and Chapin, C.E., 1997, The New Mexico Geochronological Database: New Mexico Bureau of Mines and Mineral Resources digital data series.

Wilson, D., R. Aster, J. Ni, S. Grand, M. West, W. Gao, Baldridge, W.S., Semken, S., 2005, Imaging the seismic structure of the crust and upper mantle beneath the Great Plains, Rio Grande rift, and Colorado Plateau using receiver functions, Journal of Geophysical Research, v. 110.

Wolf, R.A., Farley, K.A., Silver, L.T., 1996, Helium diffusion and low temperature thermochronology of apatite, Geochimica et Cosmochimica Acta, v. 60, p. 4231-4230.

Appendix 1: Sample locations and corresponding AFT dates

Sample	Latitude	Longitude	Elevation (m)	AFT pooled age (Ma)	AFT 2σ error (Ma)
L09-BL4	39.7199'	-106.1990'	3016	-	-
L09-H92	39.5618'	-106.0849'	2853	-	-
MP97-289	39.7689'	-106.2892'	3011	14.1	1.9
GRWL1	39.6917'	-106.2181'	3911	15.9	2.2
GRWL2	39.6953'	-106.2150'	3755	13.5	2.2
GRWL3	39.6942'	-106.2114'	3603	16.8	3.4
GRWL8	39.6917'	-106.2019'	3230	11.7	2.0
L09-BL3	39.7133'	-106.2187'	3201	-	-
L09-BL2	39.7125'	-106.2171'	3102	-	-
GRF1	39.5750'	-106.1131'	2791	7.5	1.6
MP97-284	39.7600'	-106.3403'	4139	24.4	2.5
MP97-287	39.7542'	-106.3358'	3658	22.4	2.2
GRVP14	39.5600'	-106.1969'	3716	32.6	4.6
GRWL12	39.6514'	-106.2425'	3746	28.9	3.1
GRWL10	39.6253'	-106.2194'	3032	21.0	2.5

AFT data from Naeser et al., 2002.
All samples with AFT dates were kindly provided for (U-Th)/He analysis by C. Naeser.